AD_____

Award Number: DAMD17-03-1-0178

TITLE: Undergraduate Training in Mammary Gland Biology and Breast Cancer

PRINCIPAL INVESTIGATOR: Mina J. Bissell, Ph.D.

CONTRACTING ORGANIZATION: Lawrence Berkeley Laboratory
Berkeley, CA 94720

REPORT DATE: May 2006

TYPE OF REPORT: Annual Summary

PREPARED FOR: U.S. Army Medical Research and Materiel Command
Fort Detrick, Maryland 21702-5012

REPORT DOCUMENTATION PAGE

Form Approved
OMB No. 0704-0188

1. REPORT DATE	**2. REPORT TYPE**	**3. DATES COVERED**
01-05-2006	Annual Summary	1 May 2003 – 30 Apr 2006

4. TITLE AND SUBTITLE

Undergraduate Training in Mammary Gland Biology and Breast Cancer

5a. CONTRACT NUMBER

5b. GRANT NUMBER
DAMD17-03-1-0178

5c. PROGRAM ELEMENT NUMBER

6. AUTHOR(S)

Mina J. Bissell, Ph.D.

5d. PROJECT NUMBER

5e. TASK NUMBER

5f. WORK UNIT NUMBER

7. PERFORMING ORGANIZATION NAME(S) AND ADDRESS(ES)

Lawrence Berkeley Laboratory
Berkeley, CA 94720

8. PERFORMING ORGANIZATION REPORT NUMBER

9. SPONSORING / MONITORING AGENCY NAME(S) AND ADDRESS(ES)
U.S. Army Medical Research and Materiel Command
Fort Detrick, Maryland 21702-5012

10. SPONSOR/MONITOR'S ACRONYM(S)

11. SPONSOR/MONITOR'S REPORT NUMBER(S)

12. DISTRIBUTION / AVAILABILITY STATEMENT
Approved for Public Release; Distribution Unlimited

13. SUPPLEMENTARY NOTES

14. ABSTRACT
NOT PROVIDED

15. SUBJECT TERMS
Breast Cancer

16. SECURITY CLASSIFICATION OF:				**18. NUMBER OF PAGES**	**19a. NAME OF RESPONSIBLE PERSON**
					USAMRMC
a. REPORT	**b. ABSTRACT**	**c. THIS PAGE**			**19b. TELEPHONE NUMBER** *(include area code)*
U	U	U	UU	45	

Standard Form 298 (Rev. 8-98)
Prescribed by ANSI Std. Z39.18

Table of Contents

SUMMARY

This research report describes the third and final year of the BCRT undergraduate research training program in breast cancer. The goal of this project was to provide undergraduate trainees with exposure to areas of breast cancer research that focus on the role of microenvironment in mammary gland biology and in the development of neoplasia. Trainees in this project benefited from working in a program that investigates the intersection of hormones, growth factors, and extracellular matrix (ECM) signaling and remodeling during mammary gland morphogenesis, differentiation, and carcinogenesis. The program was advertised through several undergraduate research forums on the UC Berkeley campus, and more than forty applications were received. From these, eight applicants were selected to represent a balance of interests and approaches, with broad levels of expertise ranging from laboratory novices to students with many years of laboratory experience. During the research portion of the program, undergraduate trainees had frequent interaction with mentors and with advanced postdoctoral fellows, and reports were presented in organized, biweekly meetings structured to reflect the organization of a research paper. At the first meeting, the students presented the introduction to their research project; at the second, the materials and methods; at the third, the results. For the final meeting of the program, the students presented their work in complete form, including conclusions and interpretations. While the success at obtaining experimental results within the allotted time of the research program varies, all the participants (both students and preceptors) agreed that the overall experience was successful.

BODY

In this section, research accomplishments of individual undergraduates will be summarized, with an emphasis on the forward direction of the projects.

Andrew Lee
Satyabrata Nandi Lab
Supervisor: Ed Blank
Project Title: Real Time RT-PCR Analysis of Estrogen-Induced Protection Against Breast Cancer

Introduction

In 1713, the Italian physician, Bernardino Ramazzin, observed that nuns had higher rates of breast cancer than most other women. In 1970, MacMahon et al. showed that across ethnic groups, women show drastic reductions in breast cancer rates if they undergo a full-term pregnancy before age the age of 20. This phenomenon has also been observed in animal models. Studies have demonstrated that rats exposed to carcinogens either before or after a full-term pregnancy have a much lower rate of mammary carcinogenesis. Similar experiments in mice show that undergoing a full-term pregnancy drastically lowers the rate of mammary carcinogenesis compared to nulliparous animals.

The protection against breast cancer conferred by early pregnancy has been the focus of many preventive strategies under development. Earlier studies have attempted to mimic the protective

effect of pregnancy against breast cancer with hormonal treatments. Treatment with high levels of estrogen and progesterone either before or after rats have been exposed to carcinogens has been shown to be highly protective against mammary carcinogenesis. Our lab has previously demonstrated that short-term treatment with levels of estrogen comparable to that at pregnancy is able to confer protection against chemically induced carcinogenesis in rats.

Despite the strong epidemiological, clinical and experimental evidence indicating the ability of hormones to protect against carcinogenesis, very little is known about the physiological and molecular mechanisms responsible for this pregnancy-induced protection. In an earlier study done by D'Cruz et al, rats were divided into parous and nulliparous groups, then RNA was extracted from their mammary tissues and analyzed by microarray. The two groups were differentiable by 38 genes that were significantly up- or down-regulated.

To understand the molecular bases of the protective effect conferred by hormonal treatment, we utilized quantitative RT-PCR to identify genes either significantly up- or down-regulated by estrogen treatments in rats. By identifying changes in the patterns of gene expression, we may be able to use these genes as biomarkers to analyze the success or failure of future hormone treatments.

Materials and Methods

Animals:
Virgin Lewis rats were purchased from Charles River Laboratories. Rats were housed in a temperature-controlled room with a 12 hour light/dark schedule and were fed food and water ad libitum.

Estradiol treatment:
All doses of estradiol were packed in individual silastic capsules in a cellulose matrix. Control animals received silastic capsules containing only cellulose. All silastic capsules were dorsally implanted, and all capsules were primed before implantation by soaking in media 199 overnight at 37°C.

Persistent effect of different doses of estradiol on gene expressions in the mammary gland:
At 9 weeks of age, rats were divided into 3 groups, each group consisting of 3 rats and receiving one of the following treatments: 1) control, 2) 10 μg estradiol, or 3) 200 μg estradiol. Each treatment was continued for 3 weeks and at the end of the treatment, the silastic capsules were removed from the animals. Eight weeks after the removal of the hormone treatment the rats were terminated and mammary glands were removed and immediately snap-frozen in liquid nitrogen and stored at -80°C.

RNA isolation:
The mammary tissues stored at -80°C were used for RNA isolation. RNA was isolated using Trizol. Total RNA was then subjected to DNase treatment and further purified with RNeasy columns. The quality of RNA was analyzed using the Agilent 2100 Bioanalyzer and quantified using a Hitachi UV spectrophotometer.

Quantitative RT-PCR:
Using RT-PCR kits from Qiagen, several genes of interest were analyzed using the RNA extracted from the rat mammary tissues. The percent changes in gene expression were calculated and significance was determined by the Student's T-test.

Results

Quantitative RT-PCR analysis of short-term estradiol changes in gene expression
The goal of this study was to confirm the efficacy of preventive estradiol treatments on genes associated with breast cancer. In an earlier study, microarray analysis identified approximately 20 genes that significantly changed expression between rats that were parous and nulliparous. We have begun examining the expression level changes in these particular genes by real time RT-PCR after treating rats with pregnancy-comparable levels of estrogen. Data generated by real time RT-PCR was used to calculate differences in the amount of mRNA present in each category.

We have run multiple quantitative RT-PCR tests on a number of genes (Table 1). Expression levels of genes of interest were normalized to β-actin levels. The 10 μg estrogen treatment group showed no significant changes in levels of expression in any of the genes of interest. This demonstrated that the 10 μg estrogen dosage did not have any protective effect on the mammary tissues. Changes in gene expression by a percentage level were calculated and then graphed (Figure 1). Superoxide Dismutase-3, Pleiotrophin, and Cluster of Differentiation 47 were shown to be upregulated, while CDK Inhibitor 1B (P27) was downregulated. However, after performing student-T-tests to determine significance, only Pleiotrophin was shown to have had its expression significantly upregulated.

Gene	Symbol	Function
CDK Inhibitor 1B	P27	Cell cycle control
Cluster of Differentiation 47	CD47	Pro-apoptotic
Superoxide Dismutase-3	SOD-3	Oxidoreductase, cell protection against degradation
β-Casein	β-Casein	Mammary cell differentiation
Pleiotrophin	Pto	Cell differentiation
Vascular Endothelial Growth Factor	VEGF	Blood vessel formation
B-Cell #2	Bcl2	Anti-apoptotic

Table 1. Genes of Interest

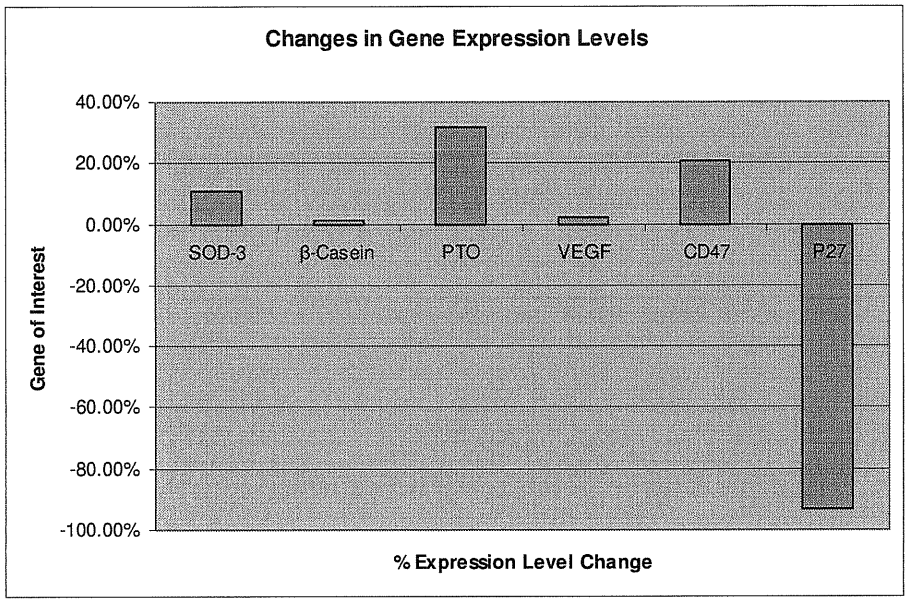

Figure 1. Changes in Gene Expression Levels

Discussion and Conclusion

The data from the current study demonstrates that Pleiotrophin has its gene expression level significantly upregulated in mammary tissues after treatment with protective high-dosages of estrogen. However, some genes that were found to have changed expression level during pregnancy are not associated with the mechanism of estrogen-induced protection against breast cancer. CDK Inhibitor 1B (P27), Cluster of Differentiation 47, Superoxide Dismutase-3, β-Casein, Vascular Endothelial Growth Factor, and B-Cell #2 were all shown to have not changed their expression levels significantly, either up or down. While it is established that treatment with pregnancy levels of estrogen confers protection against mammary carcinogenesis, the mechanism of this protection is not clear. The data obtained from this experiment will be helpful in understanding the mechanisms involved in estrogen-induced protection and will also help identify biomarkers associated with this protective process.

Acknowledgements

I would like to thank Derek Radisky and other organizers of the BCRT Summer Program for giving me this opportunity to do research. I would like to thank Ed Blank and the other members of the Nandi Lab who taught me the lab techniques I used all summer and guided the course of my project. This program was sponsored by U.S Army Grant # DAMD17-03-1-0178

References

1. Kurtz A, Spitzer E, et al. Local control of mammary gland differentiation: mammary-derived growth inhibitor and pleiotrophin. Biochem. Soc. Symp. Great Britain 2002; 63: 51-69

2. D'Cruz CM, Moody SE, Master SR, et al. Persistent parity-induced changes in growth factors, TGF-beta 3, and differentiation in the roden mammary gland. Molecular Endocrinology 2002; 16:2034-2051
3. Rajkumar L, Guzman RC, Yang J, et al. Short-term exposure to pregnancy levels of estrogen prevents mammary carcinogenesis, Proc. National Academy of Science USA 2001; 98: 11755-11759
4. Guzman RC, Yang J, Rajkumar L, et al. Hormonal prevention of breast cancer: Mimicking the protective effect of pregnancy. Proc. National Academy of Science USA 1999; 96: 2520-2525

Carol Li
Mina Bissell Lab
Supervisor: Celeste Nelson
Project Title: Branching Morphogenesis: A TGF-β Responsive Promoter Reporter Construction

Abstract

The initial understanding of the normal cells' nature and fundamental processes is essential to gaining perspective on the various conditions and causes of cancer. In an attempt to study breast cancer, a discussion of the methods in constructing a transforming growth factor- β (TGF-β) responsive promoter reporter in relation to branching morphogenesis will follow. Using the obtained successful constructs, further transfection and incorporation into a three-dimensional (3D) model of mammary epithelial cells in culture will be performed. Future experiments involving the treatment of the transfected cells with TGF-β will guide our understanding of what role this pathway plays and what effect it has on cells in branching morphogenesis.

Introduction

To better understand the nature of breast cancer, it is necessary to strengthen our knowledge of the normal epithelial growth that drives mammary gland development. Morphogenesis in the mammary gland consists of an expansion and branching of the ductal system in a predictable pattern. Because the normal signaling and branching that regulate mammary epithelial growth are disrupted during the progression of cancer, the purpose of this project is to examine the nature and function of these signals in a normal environment using a realistic three-dimensional (3D) model of mouse mammary epithelial cells in culture. The signaling pathway of interest is driven by TGF-β, a transforming growth factor that is believed to inhibit and/or promote epithelial growth in mammary development. The main goal is to localize TGF-β responsive areas in populations of cells after transfection within a culture model of the mammary gland for 3D visualization. In the end, a more affirmative relationship between TGF-β and branching morphogenesis can be deduced and tied to the stimulation of epithelial-mesenchymal transition (EMT), a process required during normal development that cancer cells undergo during metastasis. This could lead to a more enriched knowledge of how to alleviate the effects of cancer in attempt to decrease morbidity.

Materials and Methods

Cell Culture
EpH4 mouse mammary epithelial cells were maintained in DMEM/F12 supplemented with 2% FCS, gentamycin, and insulin as previously described (Reichmann et al., 1989).

Construction of reporter plasmid
The luciferase reporter gene, p3TP-lux, was selected for its highly TGF-β responsive regions: 3 TPA response elements, TREs, and plasminogen activator inhibitor 1, PAI-1 (Wrans et al., 1992). The TGF-β responsive 3TP promoter was PCR amplified from p3TP-lux (obtained from Kunxin Luo, UCB) using the primers 5'-GCT AGC TCG AGC AGC TGA AGC TCC CTT CCA-3'and 5'-GAG GAA TTC GAG CTC GGT ACC CCG ACA CGG-3' and 5'-GAG CCG CGG GAG CTC GGT ACC CCG ACA CGG-3', containing embedded XhoI, EcoRI, and SacII sites (Fig. 1).

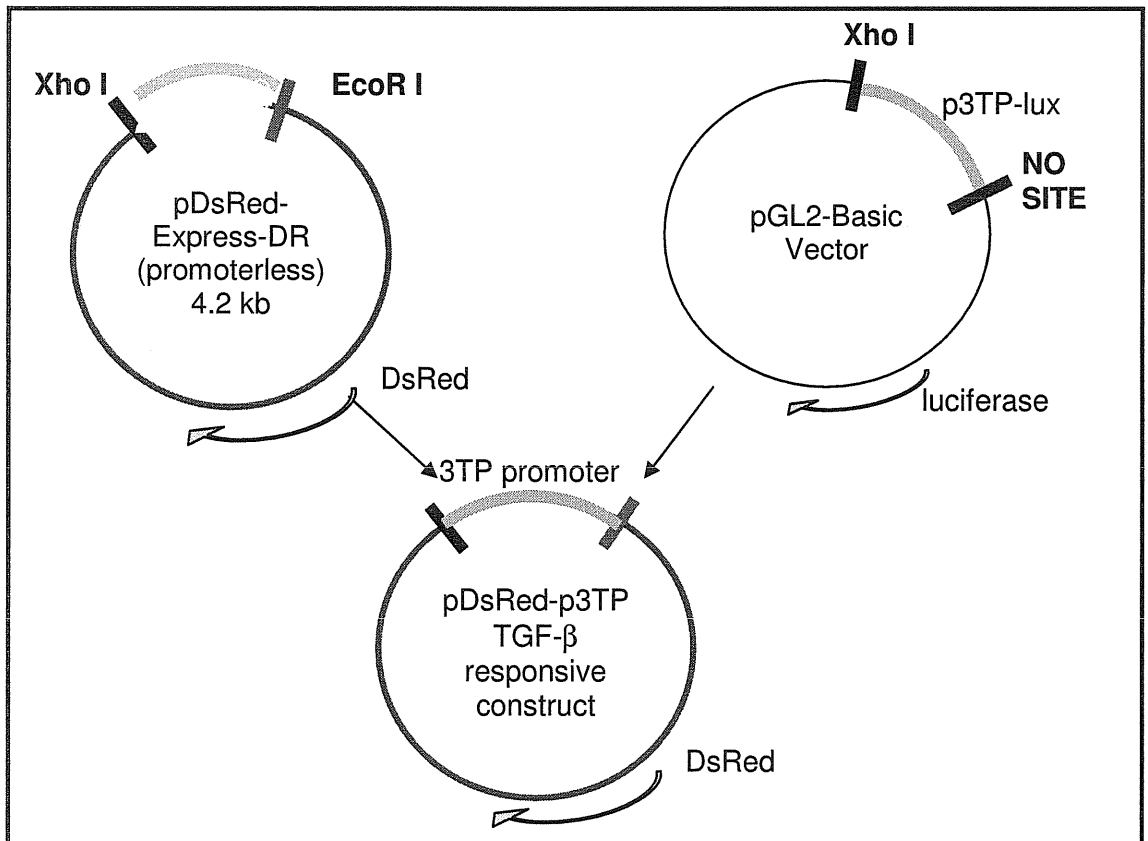

Fig. 1. The above display is a model of the experimental design for this project. The ultimate goal is to form the pDsRed-p3TP TGF-β responsive construct as illustrated above.

The vector pDsRed-Express-DR (Clontech, Mountain View, CA) and resulting PCR products were sequence verified, digested, ligated and transformed. The recombinant plasmid DsRed-3TP was transfected into EpH4 mouse mammary epithelial cells, which were stably selected with

Neomycin. Red fluorescence will be observed upon treating the mammary epithelial cells with TGF-β.

Results

Ligation of p3TP-lux insert and DsRed vector was confirmed by the presence of colonies on plates treated with kanamycin and each transformation mixture containing DNA with XhoI-EcoRI and XhoI-SacII ligation sites. The number of colonies on EcoRI ligated p3TP-DsRed plates far exceeded the colonies on SacII ligated p3TP-dsRed plates, thus allowing up to seven colonies to be selected from the aforementioned plates and cultured overnight in round-bottom tubes. Diagnostic digests of minipreps from overnight culture were performed and later visualized using gel electrophoresis techniques. The resulting bands from this process exhibited faulty cuts or no cuts at all. To check the possibility of colonies with good DNA from the remaining colonies, another stock of minipreps and diagnostic digests was performed under the same conditions with newly picked colonies. Another gel electrophoresis of diagnostic digest for all 15 of the resulting minipreps displayed appropriate cuts for colonies 1-3, 5, 6 (EcoRI) and 5,7 (SacII) as shown in Fig. 2 and 3.

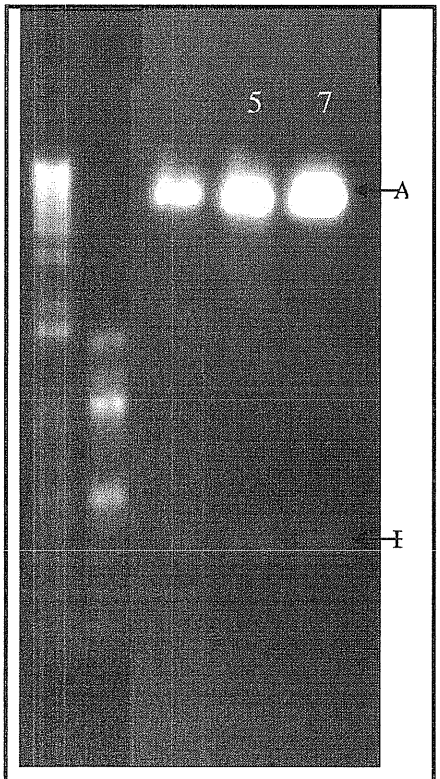

Figure 2. Comparing with a 1 kb and 100 bp marker, respectively, colonies of SacII 5 and 7 clearly show appropriate bands at 4.2 kb (A) and ~300 bp (B) to indicate successful ligations.

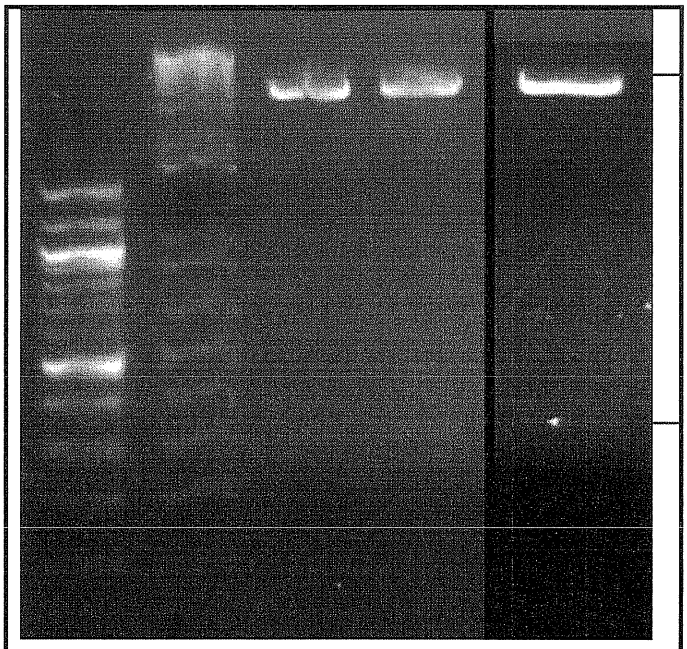

Figure 3. EcoRI 1,2, and 6 all show the appropriate cuts (with a significantly faint second band) at the right positions—emphasized by the red arrows—when compared to the 100 bp and 1 kb ladders shown on the far left.

To prepare enough DNA for transfection of mammary epithelial cells, Qiagen's midiprep kit for high-copy plasmids was used to purify the DNA from SacII overnight cultures 5 and 7. After transfecting the EpH4 mammary epithelial cells with the purified recombinant DNA, the cells did indeed shine red under fluorescence. In addition, co-transfection with a dominant recessive TGFβII receptor to block TGFβ signaling yielded a smaller number of red fluorescence cells,

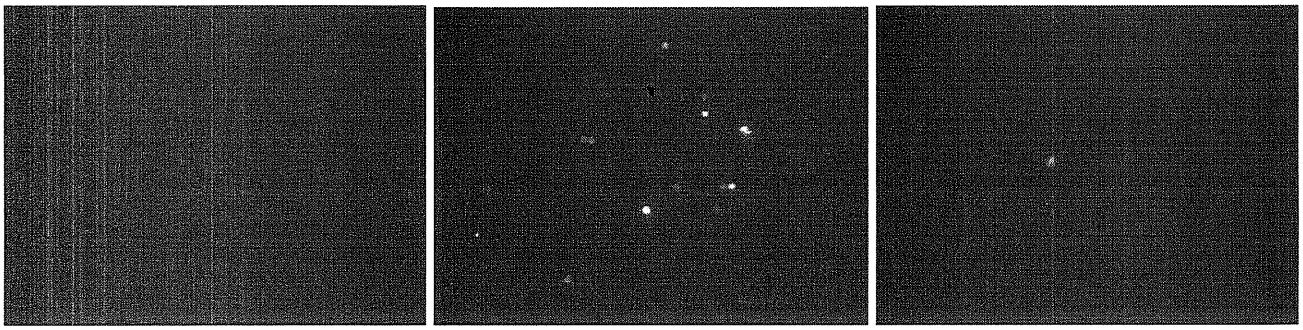

Figure 4. EpH4 Mouse Mammary Epithelial Cell Transfections with TGF-β Responsive Construct, pDsRed-3TP-Sac 5
(Left) Transfected EpH4 with DsRed as a control; thus, no red cells were visible.
(Middle) Transfection with pDsRed-3TP-Sac 5; red cells were clearly visible.
(Right) Co-transfection of pDsRed-3TP-Sac 5 and TGF-β receptor, +/- DNTbR II; fewer red cells are shown.

which suggested a successful p3TP-dsRed-XhoI-SacII construct (Fig. 4).

DNA of 3TP-dsRed-Sac 5, p3TP-dsRed-Sac 7, p3TP-dsRed-EcoRI-1,2, and 6 was quantified and sent to SeqWright for sequence verification. The obtained sequencing report for the Sac II samples showed no defects. However, the sequencing report for EcoRI samples calls for more investigation.

Summary

I report here the establishment of successful TGF-β responsive p3TP promoter constructs and subsequent transfections of EpH4 mouse mammary epithelial cells. Further treatment of the cells with TGF-β is still in progress; thus, no solid conclusion could be drawn about the relationship between branching morphogenesis and TGF-β. There is still much to learn about what specific role TGF-β plays in a cellular context. The progression of these studies and experiments will lead us closer to a better understanding of breast cancer and other cancerous growths. Future experiments involving use of a different reporter and more controls are also being considered for means of improvement towards this project.

Acknowledgements

I thank Derek Radisky, Dr. Mina J. Bissell, and the Breast Cancer Research Training (BCRT) program for giving me the opportunity for taking part in this summer research program. I thank Celeste M. Nelson for her guidance in mentorship. I thank the Bissell laboratory for providing all

necessary materials. This work is supported by the Department of Defense (DAMD17-03-1-0178).

References

Riechmann, E., Ball R., Groner B., and Friis R.R. (1989). New Mammary Epithelial and Fibroblastic Cell Clones in Coculture Form Structures Competent to Differentiate Functionally.*The Journal of Cell Biology*. 108: 1127-1138.

Wrans, J. L., Attisano L., Carcarno J., Zentella A., Doody J., Laiho M., Wang X.F., and Massague, J. (1992). TGFβ Signals Through a Heteromeric Protein Kinase Receptor Complex. *Cell*. 71: 1003-1014.

Deepti Nahar
Mina Bissell Lab
Supervisor: Aylin Rizki

Project Title: The Role of Breast Cell Microenvironment in DNA Repair Gene Expression

Introduction

The microenvironment of a cell can have significant effects on gene expression. The primary focus of this project will be to compare gene expression levels between cells grown in 2D and 3D-lrBM, with particular emphasis on DNA repair genes. 2D cells are grown on tissue culture plastic, whereas 3D-lrBM cells are grown in reconstituted basement membrane, such as Matrigel. The 3D environment is designed to mimic the extracellular matrix that surrounds the breast epithelium *in vivo*. Specifically, it is rich in laminin, which regulates morphological differentiation of cells grown in such an environment. Thus, cells grown in Matrigel have the ability to form polarized structures with a central lumen, reflecting the nature of cells *in vivo,* while cells grown in a 2D environment don't share this ability to represent the *in vivo* organizational structure of cells. How the microenvironment affects DNA repair is of particular interest because we have recently shown that cells grown in 3D-lrBM have altered double-strand break repair characteristics than cells grown in 2D tissue culture plastic(unpublished).

Previously, we compared global mRNA levels between non-tumorigenic human breast epithelial cells, from the HMT-3522-S1 cell line, grown in 2D vs. 3D using microarray hybridizations on LBNL slides containing 8000 genes. Using GenePixPro and GeneSpring software, raw ratios were determined and normalized to the entire slide. A list of statistically differentially expressed genes was created with a t-test, p-value < 0.05. From this list, genes that are involved in double-strand break repair, were/are being confirmed via both quantitative and semi-quantitative RT-PCR (Real Time Polymerase Chain Reaction). We are especially focusing on the MRN complex, a complex comprised of the genes MRE11, RAD50, and NBS1. Further work will be conducted to determine whether changes due to the environment a cell is grown under observed at the mRNA level is also maintained at the protein level. This goal will be achieved by determining the amount of protein via Western blots. To determine whether differences are due to signaling form the extracellular matrix or not, we will be doing an experiment in which single

plated cells are allowed to attach to plastic, and then some samples will have 10% Matrigel added to them, to reflect the extracellular matrix component.

Materials and Methods

To verify the results of the microarray experiments, we will be using semi-quantitative reverse-transcription Polymerase Chain Reaction (RT-PCR). To measure the level of mRNA in a given sample, conditions for primers, which are designed to specifically recognize the target gene, will be optimized by using sample cDNAs and testing using various conditions. Parameters that we will alter to determine the most optimum conditions include the annealing temperature, the number of cycles, the duration of each step in the PCR cycle, and the concentration of MgCl2. After determining the conditions that give the best results, we will use those conditions for future experiments with that set of primers. This needs to be done for each set of primers that will recognize a particular gene. Using the designed primers and the optimized conditions for the primers, we will measure the mRNA expression levels of those genes in prepared cDNA samples. The cDNA samples are from cells which were growth arrested on day 8 from a 10-day culture by removing EGF. These S1 cells from the HMT-3522 cell line were grown in either a 2D environment (two samples) or from a 3D-lrBM environment (two samples). After running the completed PCR reaction samples on a .9-1.0 % agarose gel, we will measure the amount of product by using spot densitometry with a ChemiImager. Taking the integrated Density values (IDV) of each sample, we will quantify the results. The reactions will be duplicated to ensure accuracy and the results will be normalized to a control gene, GAPDH. These results will be compared to those from the microarray to verify the data we obtained from them.

To determine whether differences in gene expression levels between samples grown in different environments are upheld at the protein level or not, we will be doing Western Blots to measure the level of protein in samples. Using protein lysates from S1 cells in different passages (passage 54, 55, and 57) that have been controlled for growth by removing EGF on day 8, we will measure the amount of protein using specific antibodies. We will study the expression level differences between cells that have been grown in a 2D environment versus cells that have been grown in a 3D-lrBM environment. Using standard Western Blot techniques to determine the amount of the selected protein, we will quantify the results by using spot densitometry and measuring the integrated density values with a ChemiImager. The results will be normalized to an internal control, Beta-Actin.

Differences observed in the expression level of selected proteins could be due to signaling from the extracellular matrix as well as from interactions between cells that arise due to the polarized acini that cells form when grown in a 3D environment. To test whether differences are due to cell structure or due to signaling from the extracellular matrix, we will conduct an experiment in which the all the cells are plated as single cells in a tissue culture plastic flask after being grown for six days in the presence of EGF. On day 6, EGF will be removed and the single cells will be allowed to attach to the plastic flask for two hours, after which some of the samples will have 10% Matrigel added to them for six hours. Differences between the samples with the 10% Matrigel treatment and the ones without the 10% Matrigel treatment are supposed to measure differences due to signaling from the extracellular matrix, since all the cells are plated as single cells and hence don't have the cell-cell interaction that is present in cells grown in a monolayer

or grown in a 3D-lrBM environment. Additionally, to assess the role of Beta-1 Integrin, we will perform a treatment to some of the samples in which we will block signaling via Beta-1 Integrin from the extracellular matrix. We will add Beta-1 Integrin Blocking Antibody to some samples that have the 10% Matrigel treatment described previously as well as to some samples that don't have the 10% Matrigel treatment, and let the antibody interact with the cells for six hours. After six hours, the cells will be harvested. 2D samples will be trypsinized to get a cell pellet that will be used to get protein lysates. For samples with the 10% Matrigel treatment, cells from the 2D layer will be trypsinized and combined with dispased cells from the 3D (Matrigel) layer. Upon extracting the protein from the cells, a Bradford Assay will be done to measure the amount of protein and determine how much protein to use for Western Blots. Protein specific antibodies will bind to the selected protein and using ChemiImager, the results will be quantified using integrated density values and spot densitometry. The results will be normalized to an internal control Beta-Actin.

Results and Discussion

Expression level differences at the mRNA level

Microarray Results
Experiments testing differences in mRNA level were done using microarrays and fluorescently labeled cDNAs. A list of genes involved in double-strand break repair that were differentially expressed and were statistically significant was generated. The microarrays examined the mRNA levels of genes of cells that were either grown in a laminin-rich basement membrane (3D-lrBM), on plastic forming a monolayer (2D), or in collagen (3D-col). Three sets of gene lists were generated, one each for the following comparisons: a)3D-lrBM vs. 2D, b)3D-col vs. 2D, and c)3D-lrBM vs. 3D-col (see Figure 1.)

3D LrBM vs 2D		3D collagen vs 2D		3D LrBM vs 3D col	
ADPRT	1.48490	XRCC3	0.874475	WRN	0.804059
RAD50	1.26790	NBS1	0.799435	DDB1	0.794435
TP53BP1	0.75419	Results verified with PCR			
TP53BP2	0.74574	→ Altered mRNA levels			
RAD52	0.78408				

Figure 1. Microarray Results with expression level ratios of selected genes involved in DSBR

Genes that were expressed differently between 3D-lrBM and 3D-col were: ADPRT, RAD50, 53BP1, 53BP2, and RAD52. ADPRT and RAD50 mRNA levels were higher in cells grown in a 3D-lrBM environment, with the fold difference values of 1.485 and 1.268, respectively. The P-values from a t-test are .003 and .029 respectively for ADPRT and RAD50, which shows that the difference is statistically significant since the value is less than .05. Conversely, 53BP1, 53BP2, and RAD52 had lower mRNA levels when grown in a 3D-lrBM environment as compared to 2D

monolayer. The fold difference values were .754, .746, and .784, respectively for 53BP1, 53BP2, and RAD52, with the respective P-values being .014, .033, and .037. Fold difference values less than 1 signify that levels were lower in 3d-lrBM as compared to 2D.

Genes that were differentially expressed between 3D-col and 2D were: XRCC3 and NBS1. Both were observed to be lower in 3D-col samples, with fold difference values of .874 and .799 and P-values of .026 and .024 for XRCC3 and NBS1, respectively.

Genes differentially expressed between 3D-lrBM and 3D-col were: WRN and DDB1. Both WRN and DDB1 had lower levels in 3D-lrBM compared to 3D-col, with fold difference values of .804 and .794 and P-values of .002 and .030, respectively.

NOTE: The cells from which mRNA was extracted for the microarray experiments were not controlled for growth by removing EGF from the media on day 8. Hence, some differences observed in the microarray results could be due to the different cell cycle the cell was in, rather than being due to the environment the cell was grown in.

PCR confirmation

The results of the microarray experiments were evaluated and verified by making cDNA from mRNA of cells that had been growth arrested on day 8 by the removal of EGF from the media for S1 cells. Experiments testing the difference in mRNA levels between cells grown in a 2D environment and cells grown in a 3D-lrBM environment were carried out by extracting the mRNA from the cells and then using reverse transcription to obtain cDNAs. The results were normalized to GAPDH. The cDNAs were then used to verify the microarray results using polymerase chain reaction (PCR) and conditions specific for the primers that were used to amplify the gene of interest.

ADPRT

Testing mRNA levels of cells grown in 3D-lrBM versus 2D through PCR confirmed microarray results. After repeating the experiment, it was determined that ADPRT levels were higher in 3D-lrBM samples compared to 2D samples. The difference was small, like the microarray data, with 3D-lrBM samples being an average of 1.208 fold higher than 2D samples.

RAD50

PCR results confirmed microarray results. RAD50 was expressed at a higher level in 3D-lrBM samples compared to 2D samples, with 3D-lrBM samples being 1.12 fold higher. This is in accordance with the microarray results since the difference for ADPRT for cells grown in 3D-lrBM versus 2D is higher than the difference for RAD50.

53BP1

PCR results were opposite the results obtained from microarray analysis. Microarrays showed 53BP1 being lower in 3D-lrBM with a fold difference of .754, whereas PCR showed 53BP1 being slightly higher in 3D-lrBM, with a fold difference of 1.117. The contradiction in results could be due to the fact that cells were not growth arrested on day 8 in the microarray results, hence the data did not account for growth differences, whereas cells for the PCR results were growth arrested on day 8. Another reason could be that microarray data could be ambiguous

since thousands of genes are compared on the same slide and it is well known that technical errors, such as a mislabeled spot, can cause such problems – thus, the need for RT-PCR quantification.

53BP2
PCR results supported microarray results. Cells grown in a 3D-lrBM environment expressed lower levels of 53BP2 than cells grown in a 2D environment. The fold difference value was .818, signifying that 53BP2 levels are higher in 2D.

NBS1
NBS1 was not among one of the genes that was differentially expressed at a statistically significant level between cells grown in 3D-lrBM and those grown in 2D in the microarray analysis. However, based on the microarray results, levels of NBS1 were higher in 2D samples compared to 3D-col samples. Using PCR to amplify NBS1, it was determined that mRNA levels of NBS1 were higher in cells that were grown in 3D-lrBM versus cells that were grown in 2D. NBS1 was 1.359 fold higher in 3D compared to 2D samples. It is not uncommon for microarrays to miss differences due to the known internal technical errors associated with the technique.

DDB1
Differences in the expression level of DDB1 was observed between cells that were grown in either 3D-lrBM or 3D-col, with levels being higher in 3D-col. This gene was not differentially expressed at a statistically significant level between cells grown in 3D-lrBM and 2D. PCR data supports this result, since there is no significant difference in the mRNA expression levels of DDB1 between cells grown in 3D-lrBM and 2D.

Expression level differences at the protein level

Three sets of lysates prepared at different times were used to detect differences in the expression levels of RAD50 and MRE11 at the protein level. This was done using standard conditions for Western Blots. Differences were observed for both RAD50 and MRE11 depending on whether the cells were grown in 3D-lrBM or plated in 2D tissue culture plastic. Effects of growth were controlled for by removing EGF on day 8 of the first two sets of lysates. Thus, the differences seen in the blots should be due to differences due to the microenvironment of the cell and not because the cells were in different phases of the cell cycle when they were harvested. The third set of lysates were used to detect the effects that Beta-1 integrin played in the regulation of genes involved in double-strand break repair (based on unpublished results that show beta1 integrin to be involved in lrBM to nucleus signaling that controls double-strand break repair). The 10% Matrigel treatment was used to compare whether the differences were due to actual interactions with the extracellular matrix or whether they were a result of whether cells were able to form acini or not.

Passage dependency
Differences in the levels of protein of MRE11 are dependent on which passage of S1 cells are used. In other words, the trends in expression levels of MRE11 are different depending on the passage that the cells are from. For cells from passage 57, levels of MRE11 were an average of 2 fold higher in 2D samples compared to 3D-lrBM samples. However, this trend was the

opposite for cells from passage 55, in which levels of MRE11 were an average of 3 fold higher for 3D-lrBM samples. The differences between the two experiments using different passage cells are not due to passage 55 and passage 57 cells' level of growth, since EGF was removed on day 8 from a 10-day culture for both sets of cells, from passage 55 and passage 57. The removal of EGF stops growth completely.

Differences in the level of RAD50 at the protein level were tested for. Across the passages tested, passage 54, passage 57, and passage55, RAD50 levels are higher in 2D compared to 3D-lrBM samples for passage 57, but lower in 2D for passage 54 and passage 55. For passage 57, RAD50 was 2.77 fold higher in 2D samples while it was 1.44 fold higher in 3D in passage 54 cells. The difference was greater for passage 55 cells, with 3D samples being an average of 3.87 fold higher than 3D-lrBM samples.

Effects of blocking Beta-1 integrin

To test for differences due to signaling from the extracellular matrix versus differences due to the structure that cells form, cells underwent a 10% Matrigel treatment. Single cells were plated on tissue culture plastic flasks and the cells were allowed to attach for 2 hours, after which a 10% Matrigel media was added to the '3D' samples and the samples were allowed to be incubated for six hours before being harvested and extracting protein lysates from them. Additionally, to test for the effects of Beta-1 integrin, which is known to mediate cell adhesion, a separate treatment was done in which Beta-1 integrin was blocked by using an antibody and incubating the samples, either in the presence or the absence of the antibody for six hours, before the cells were harvested.

MRE11 levels are higher for all samples that had the 10% Matrigel treatment ("3D") as opposed to cells that were grown in a regular 2D environment. This result is seen after normalization to B-Actin and the trend is present regardless of whether the cells were incubated with the Beta-1 integrin blocking antibody or not. Presence of the antibody resulted in higher levels of the MRE11 protein, as can be observed by Figure 2 below.

RAD50 levels are lower for cells that had the 10% Matrigel treatment as opposed to cells that did not receive that treatment. The difference is approximately .79 fold, signifying that RAD50 levels were higher for 2D samples than for samples with the 10% Matrigel treatment for 6 hours. This difference is seen regardless of whether the Beta-1 integrin blocking antibody is present or not. As far as the effects of the antibody itself, it appears that there is no difference in the level of RAD50 protein expression between cells that have had the Beta-1 integrin blocking antibody treatment or not. Hence, Beta-1 integrin does not seem to play a role in mediating protein expression levels of RAD50, since the presence or blockage of it did not alter results. See figure 3 below for the protein levels of RAD50 in cells that had undergone the 10% Matrigel treatment and those who did not, as well as cells that had the Beta-1 integrin blocking antibody compared to the cells that did not have the antibody.

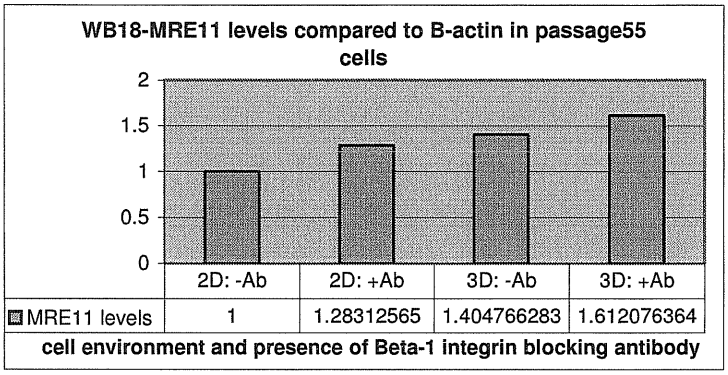

Figure 2. Protein levels of MRE11 in passage 55 cells that undergo treatment with or without Matrigel and with or without Beta-1 integrin blocking antibody.

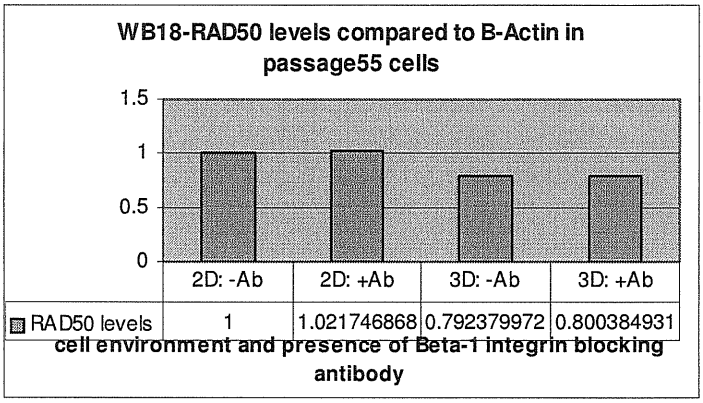

Figure 3: Protein levels of RAD50 in passage 55 cells that undergo treatment with or without Matrigel and with or without Beta-1 integrin blocking antibody.

Conclusion

Most of the differences observed at the mRNA level via microarrays were verified and confirmed through PCR. Preliminary data show that the protein expression level of RAD50 is observed to be higher for samples grown in 3D-lrBM for earlier passages, passage 54 and 55. Rad50 protein levels are lower in 3D-lrBM samples for passage 57. MRE11 protein levels are also passage dependent, with levels being higher in 3D-lrBM samples for passage 55 and lower in 3D-lrBM samples for passage 57. Blocking Beta-1 Integrin results in higher protein levels of MRE11 and has no effect on protein levels of RAD50. Differences in protein level between 2D and 3D-lrBM samples that were seen for MRE11 were due to extracellular signaling, and not just due to the organizational structure of the cells (as shown by the 10% Matrigel treatment experiment.)

Acknowledgements

I'd like to thank Mina Bissell for offering me the opportunity to be a part of her lab and Aylin Rizki for her guidance, support, supervision, and assistance. I'd also like to thank Derek Radisky for overseeing the BCRT program and the Department of Defense for funding.

Jason Ahn
Mina Bissell Lab
Supervisor: Hidetoshi Mori
Project Title: The Role of Membrane Type 1 Matrix Metalloproteinase in EpH4 Mammary Gland Morphogenesis

Abstract

It is known that matrix metalloproteinases (MMPs) play a role in extracellular matrix (ECM) remodeling. The objective of this research is to understand the function and role of membrane type-1 matriz metalloproteinase (MT1-MMP) in the normal development of mammary gland morphogenesis and differentiation. Previous studies have shown MT1-MMP upregulation in metastatic cells. We tried to determine the regulation of MT1-MMP during the branching stage of mammary gland development, and in mammary gland function. We also investigated the role of MT1-MMP in mammary gland function. This study, suggests MT1-MMP is strongly involved in the branching stage of mammary gland morphogenesis.

Introduction

Matrix metalloproteinases (MMPs) are proteolytic enzymes that regulate cell behavior in regards to remodeling cell environment (Egebald et al., 2002). The cell environment in itself has been shown to regulate cell function (Bissell et al., 2001). In most cancers MMP expression and activation is increased. MMPs can promote cancer progression by regulating cancer-cell growth, apoptosis, migration, invasion, metastasis, and angiogenesis. MMPs degrade structural components of the extracellular matrix (ECM) and also participate in release of cell-membrane-bound precursor forms of many growth factors. (Egebald et al., 2002). Growth factor receptors and cell-adhesion molecules are also MMP substrates for cleavage. In cancer, MMPs are not upregulated by gene amplification or activating mutations, so it is probably due to transcriptional changes.

During the morphogenesis and differentiation of mammary glands, a highly regulated cell proliferation and migration is conducted dynamic ECM remodeling. MMPs play a key role in the degradation and reorganization of ECM, which is a barrier for cell migration. To date, 21 enzymes have been identified as mammalian MMPs of which Membrane type 1 matrix metalloproteinase (MT1-MMP) was first identified as a specific activator for MMP-2 (gelatinase A) and also as a key molecule for cancer cell invasion and metastasis (Brinckerhoff et al., 2002). This molecule is reported as playing a role not only in ECM degradation, but also in cell proliferation, cell migration, and cell differentiation.

The mammary gland develops in stages: branching, alveolar structure formation, milk expression, and involution. (Radisky et al, 2003). It has been shown that MT1-MMP is present in mammary glands near the epithelial cells during normal development (Wiseman et al., 2003). MT1-MMP function in normal mammary gland development is not known well and we will try to understand MT1-MMP in some of the events of mammary gland development. In this research, we are investigating the roles of MT1-MMP in normal mammary gland formation, to

compare the differences between normal mammary gland development and breast cancer development.

Materials and Methods

Vectors and Transfection
We used mammalian expression vector pcDNA 3.1 (-) (Invitrogen) for expression of wild type human MT1-MMP. For RNAi we used pSuper-Neo RNAi expression vector (OligoEngine) with targeted MT1-MMP sequence. The protocol of FuGENE 6 Transfection Reagent (Roche) was used for the transfection. For selecting cells, growth media supplemented with G418 (600μg/ml) was used. After two-week selection, cells were used for the assay.

Cell Culture: EpH4 Mammary gland epithelial
EpH4 mouse mammary gland epithelial cells were maintained in DMEM/F12 supplemented with 2% fetal bovine serum, gentamycin (50μg /ml) and insulin (5mg/ml) on plastic tissue culture dish. Differentiation media (Prolactin (3μg/ml), Insulin (5μg/ml), Hydrocortisone (1μg/ml)) was used to induce beta-Casein expression.

Preparation of EpH4 cell clusters
EpH4 cell clusters were prepared as previously described (Hirai et al., 1998) with some modifications. In short, 1ml of 2% agarose in growth media was added to 8 wells of a 24 well plate and 1ml of growth media was added in the other wells to prevent dessication of the gel. After the agarose had gelled, $1x10^5$ cells suspended in 500μl of growth medium containing DNAase (1/20 final dilution) were incubated on top of the agarose with gentle rotation (100rpm) for 24 hours at 37°C. The remaining single cells were removed by centrifugation for 10 seconds at 1500 rpm.

Three-dimensional cultures
For three-dimensional cultures, EpH4 cell clusters were embedded in type I collagen gels as previously described (Hirai et al., 1998). "Acid-soluble collagen (7.5 vol of a 0.5% solution; Cellagen™ AC-5; ICN) was mixed gently on ice with 1 vol of 1.5 mM HCl (blank solution) and 1 vol of 10× DMEM/ F12, followed by mixing with 0.5 vol of alkaline solution to neutralize the pH. After adding 1:20 vol of FCS, 250 μl of the collagen solution was poured into each well of a 24-well dish, and the dish was incubated at 37°C to allow gelation of the basal collagen layer. The cell clusters were suspended in growth medium at a concentration of 2,500 to 4,000 clusters/ml, and 10 μl of the suspension (25-40 clusters) was mixed with 250 μl of ice-cold collagen solution, poured onto the basal collagen layer, and placed immediately at 37°C. After gelation of collagen, 40-80 cell clusters were added to each well and a top layer of collagen 80μl wa added and left at room temperature to gel. 200μl of chemically defined medium consisting of DMEM/F12 containing Nutridoma NS medium supplement (Boehringer Mannheim) and ITS (insulin/transferrin/selenium, Sigma). EGF (Sigma), was added to wells at a concentration of 50 ng/ml" (Hirai et al., 1998).

Analysis of branching morphogenesis
The branching phenotype of cell clusters embedded in collagen gels was determined after cultivation for 4-6 days. The branching phenotype was defined as a cell cluster having at least one process (branch) extending from its central body.

Inhibitor
The hydroxamic acid, GM6001 (3-(N-hydroxycarbamoyl)-(2R)-isobutylpropionyl-L-tryptophan methylamide) is a general inhibitor of all MMPs with K_i values of less than 100 nM (Simian et al, 2001).

RT-PCR
For cDNA synthesis, 500ng of total cellular RNA, prepared with SuperScript II (Invitrogen) according to the manufacturer's instructions. beta-casein was amplified with PCR and as a control for total RNA integrity, PCR for GAPDH was performed. The resulting amplified fragments were analyzed on 1% ethidium bromide-stained agarose gels with FluorChem Imaging Systems (San Leandro, CA).

Results

MT1-MMP enhances branching
To study branching morphogenesis we used mouse mammary gland epithelial cells, EpH4. Previously, our laboratory showed that branching in EpH4 cells could be induced by growth factors (Simian et al., 2001). Our results show that MT1-MMP expression enhances branching morphogenesis measured by the length of tubular elongation and amount of side branching (Fig.1). Without growth factors the cell clusters do not exhibit branching. With growth factors branches form, and there is increased tubular elongation and increased number of processes in the MT1-MMP expressed cell clusters.

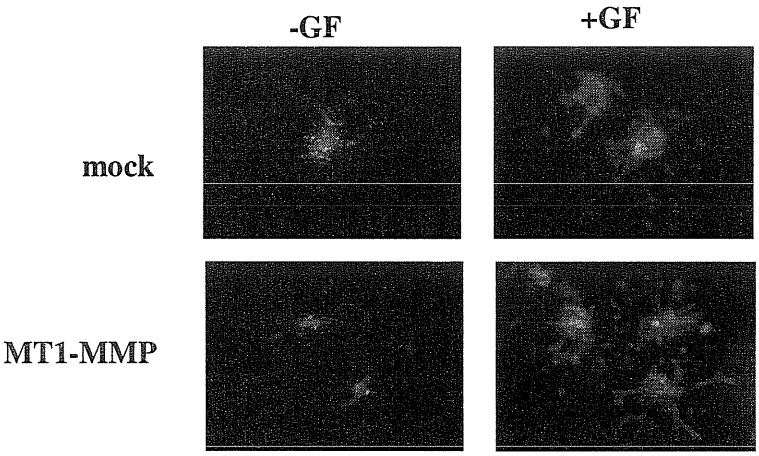

Fig. 1. MT1-MMP expression enhances branching. Live cells were stained with Calcein dye (Invitrogen). In the right column, the MT1-MMP expression increased branching phenotype.

MT1-MMP is required for branching

To understand if MT1-MMP is required for branching, RNAi silencing MT1-MMP expression was transfected. Our results show us that MT1-MMP is required for branching morphogenesis (Fig.2). As expected, the mock transfected cells show branching. The MT1-MMP RNAi transfected cells do not show branching measured by the length of tubular elongation and amount of side branching.

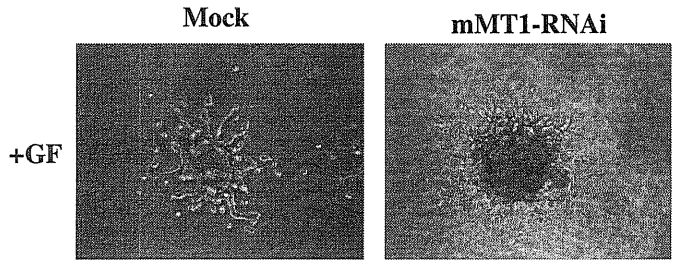

Fig. 2. MT1-MMP is required for branching morphogenesis. There is branching in the mock transfectant cells. There is no branching in the MT1-MMP RNAi cells.

MT1-MMP may be involved in beta-Casein expression

To see if MT1-MMP is involved in the functional stage of mammary gland development (lactation), we used general MMP inhibitor, GM6001 as well as specific gene MT1-MMP RNAi. The EpH4 cells onto plastic cell culture dish were treated with differentiation media. To see the role of MT1-MMP in the function of the mammary gland, the milk gene expression (beta-Casein) was measured. Our PCR results show us that MMPs as well as MT1-MMP may be involved in milk gene expression (Fig. 3). The band intensity of cells treated with GM6001 is lower than the control. The MT1-MMP RNAi expressing cells show lower band intensity than the control as well. However the difference between our control and our samples are not large enough to be conclusive.

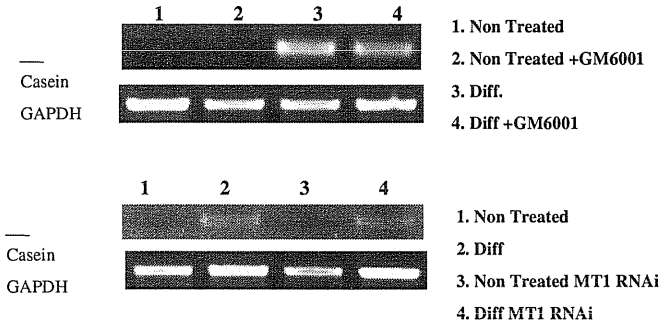

Fig. 3. MT1-MMP may be involved in beta-Casein expression. General MMP inhibitor GM6001 reduced beta-Casein expression. MT1-MMP RNAi also reduced beta-Casein expression.

Discussion and Conclusion

The goal of the present study was to delineate how MT1-MMP is involved in mammary gland developmental stage of branching as well as its functional stage of milk production. In this study we have shown that MT1-MMP enhances branching morphogenesis and is required for branching morphogenesis. MT1-MMP activity may enhance branching morphogenesis because it can locally degrade the surrounding extracellular matrix (ECM). If the surrounding ECM is degraded by MT1-MMP, invasion of epithelial cells can be facilitated. So the morphology of the MT1-MMP expressed cells exhibited more branching than the control.

The degradation of the ECM seems to be necessary for the elongation of tubes and MT1-MMP may be the key player in ECM degradation. If epithelia overexpress MT1-MMP, the surrounding ECM is more degraded. The absence of ECM, or the lessening of ECM may send signals to the cell clusters to branch, perhaps, to fill in the space. However, the control (+MT1-MMP, -EGF), shows us that a signal other than degraded ECM is necessary for branching.

On the other side of the spectrum, if MT1-MMP expression is silenced through RNAi, we see that branching does not occur. This may be the result of an unscathed ECM that does not send signals or physically allow the cell clusters to branch. However, even though the treatment with a growth factor sends signal for branching, the cell clusters do not branch when MT1-MMP is silenced. Therefore it seems that ECM degradation by MT1-MMP is necessary for branching, and ECM signaling overrides exogenous signals for branching. MT1-MMP knock out mice have been shown to develop diseases due to inadequate collagen turnover (Holmbeck, et al., 1999). This phenomenon seems to transfer over to the mammary gland because of the lack of branching even in the presence of growth factors.

It has been shown that in MT1-MMP overexpressing mice beta-Casein was not expressed (Ha et al, 2001). To understand whether this was a result of abnormally developed mammary gland, or of MT1-MMP expression itself we checked beta-Casein expression in MMP and MT1-MMP inhibited epithelial cells. According to the PCR data, it seems that MMP and MT1-MMP may be involved in the functional aspect mammary gland in beta-Casein expression. However, our data is inconclusive, in that there is only a 20% reduction in beta-Casein expression in both cases. This data suggests that in MT1-MMP overexpressed transgenic mice, beta-Casein expression is inhibited because of abnormal mammary gland development rather than because of MT1-MMP expression itself.

References

1. Bissell, M. J. & Radisky, D. Putting tumors in context. *Nature Rev. Cancer* **1**, 46-54 (2001).
2. Brinckerhoff C. E. & Matrisian L. M. Matrix metalloproteinases: a tail of a frog that became a prince. *Nature Rev. Mol Cell Biology* **3**, 207-214 (2002).
3. Egeblad, M. & Werb, Z. New functions for the matrix metalloproteinases. *Nature Rev. Cancer* **2**, 161-174 (2002).
4. Ha, H. Y. & Moon, H. B. Overexpression of Membrane-type Matrix Metalloproteinase-1 gene induces mammary gland abnormalities and adenocarcinoma. *Cancer Research* **61**, 984-990 (2001).

5. Hirai, Yohei et al. Epimorphin Functions as a Key Morphoregulator for Mammary Epithelial Cells *J. Cell Biol.*, (1998).
6. Holmbeck, K & Bianco Paolo. MT1-MMP Deficient mice develop dwarfism, osteopenia, arthritis, and connective tissue disease due to inadequate collagen turnover. *Cell* **99**, (1999).
7. Simian, M. & Hirai, Y. The interplay of matrix metalloproteinases, morphogens, and growth factors is necessary for branching of mammary epithelial cells. *Development*, **128**, (2001).
8. Radisky, D.C. & Hirai, Yohei. Delivering the message: epimorphin and mammary epithelial morphogenesis. *Trends in Cell Biology* **13,** (2003).
9. Wiseman, B.S., Site-specific inductive and inhibitory activities of MMP-2 and MMP-3 orchestrate mammary gland branching morphogenesis. *J. Cell Biol.* 162, 1123-1133 (2003).

Neda Roosta
Mina Bissell Lab
Supervisors: Jamie Bascom and Aylin Rizki
Project Title: Epimorphin in Human Mammary Epithelial Cells

Introduction

Epimorphin is a mesenchymal protein essential for epithelial morphogenesis, as discovered by Hirai et al. (1) Epimorphin expression was first found in fetal lungs and rudimentary skin cells, but has also been found to direct epithelial morphogenetic processes in mammary glands (Figure 1). Epimorphin has been significantly studied in mouse models and has been shown to play an integral role in mammary gland development by directing both luminal and branching morphogenesis (2). In fact, when epimorphin was over-expressed in mammary epithelial cells of transgenic mice, multiple outcomes were observed: precocious development, enlarged ductal lumina, delayed involution, and tumorigenesis in aged mice (3, 4). (Figure 2, 3, 4) However, it was not been determined whether epimorphin over-expression plays such roles in human mammary epithelial cells.

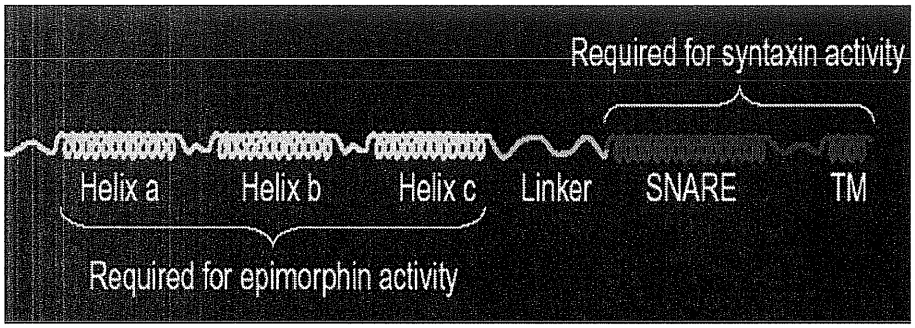

Figure 1 Epimorphin Structure: EPM is approximately 34 Kilodaltons long and has 289 amino acids. EPM lacks signal peptides that are usually found in extracellular proteins. However, it has both intracellular and extracellular functions. When localized to the extracellular face of the cell, epimorphin functions in morphogeneis. But, if localized to the intracellular face, it's involved with vesicle fusion and is called syntaxin 2. EPM has been expressed in many tissues where it has different morphogenetic functions. In normal mammary glands (non-tumorigenic), EPM stimulates both branching and luminal morphogenesis.

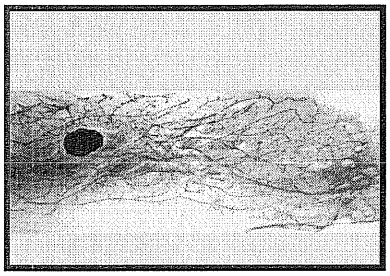

Figure 2: Wildtype Littermate Mammary Gland (Normal EPM expression)

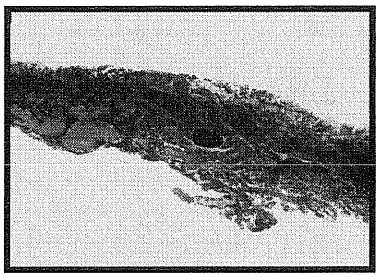

Figure 3: WAP-EPM Transgenic Mammary Gland (EPM Overexpression)

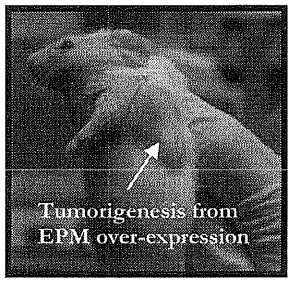

Figure 4: 18 month old WAP-EPM mouse

Human epimorphin was discovered through molecular cloning, from which its isoforms were also identified (5). This study concluded that in both mice and humans, epimorphin has three isoforms and lacks signal peptides that are usually found in extracellular localized proteins. In fact, the primary structure of human epimorphin is about 90% similar to that of the mouse (5). Therefore, our aim was to determine whether human mammary epithelial cells express epimorphin and if expression levels change depending on the tumorigenic potential of the cell lines used. By using reverse-transcriptase polymerase chain reaction (RT-PCR), we studied a human mammary epithelial progression series called HMT-3522 obtained from reduction mammoplasty (6). They proceed from S1 cells which are non malignant to T4 cells, which have tumorigenic properties. The cells can be either on a 2D plate where they form one layer cells (Figure 5), or in extracellular matrix where they form 3D structures, in an environment that is most similar to its physiological conditions (Figure 6). By using this progression series, we assessed whether epimorphin levels increase in human cells as they become more tumorigenic.

Materials and Methods

Total RNA was extracted from the HMT-3522 cell line, including non-malignant S1 cells, S2 cells, S3 mini, S3 midi, S3 maxi, and tumorigenic T4 cells. RNA was extracted using Trizol. After the medium was aspirated from cell dishes, the cells were washed with 1x PBS. Trizol was added to cells and mixed with a pipette until the solution was no longer viscous. After transferring this solution to a 15 ml polypropylene tube, the samples were centrifuged for 10 minutes at 9000 rpm at 4° C. The supernatant was transferred to a fresh tube and 20% of Chloroform for Trizol was added. Next, the tubes were vortexed for 15 seconds, sat at room temperature for 10 minutes, and were centrifuged again for 15 minutes. The supernatant was transferred to a fresh tube and 0.5 ml/ml Trizol of IPA was added as well as 0.5 µl of Glycogen/ml Trizol. The solutions were mixed, incubated at room temperature for 5-10 minutes, and centrifuged for 10 minutes. The supernatant was discarded and the samples were washed with 1 ml of 75% EtOH (RNase—free) to each tube. The dry pellet was resuspended in nuclease-free water and stored at -20°C. Quantification of RNA was determined.

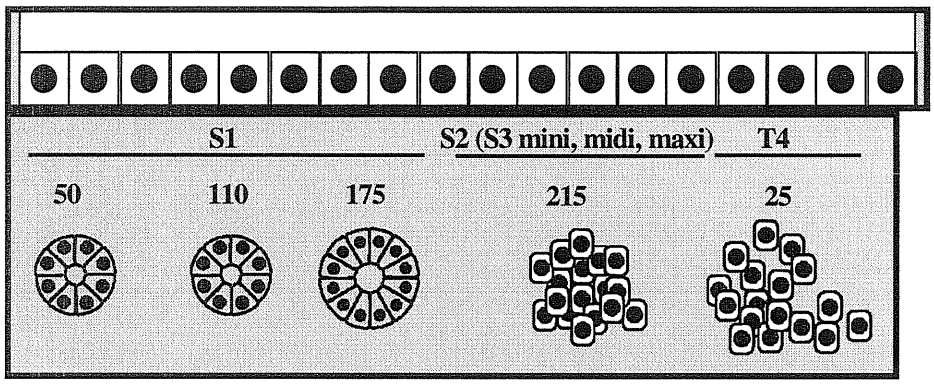

Figure 5: HMT-3522 Cell Series on 2D plates.

Figure 6: HMT-3522 Cell Series on 3D extracellular matrix.

cDNA was synthesized in order to be used in PCR reactions to determine the expression levels of epimorphin at different stages in the cell line. cDNA was created using the MMLV kit. 1 μg (4 μl) of the extracted RNA was placed in a 1.5 ml tube. 0.5 μg of primer was added per μg RNA, and the solution was raised to 15μl with water. The solution was incubated at 70°C for 10 minutes and spun briefly in a microcentrifuge. A separate solution was prepared with the following components: 10x First Strand Buffer (2.5μl), dNTP mix (1μl), MMLV RT (1μl), Oligo $dT_{19}V$ (1μl), RNA (1μg), and nuclease-free water up to a total volume of 25μL. The reaction was incubated at 37°C for 30-60 minutes. The cDNA was stored at -20°C.
Primers specific for human epimorphin were designed using PubMed. PCR was used to determine both GAPDH levels as well as epimorphin levels. A mastermix was prepared with the following components: PCR buffer 10x (2.5μl), nuclease-free water (18.3 μl), dNTP mix 10μM (0.5 μl), forward primer (0.5 μl), reverse primer (0.5 μl), $MgCl_2$ (1.5μl), and Taq polymerase (0.2μl). One μl of template was added to 24 μl of mastermix. The reaction conditions of PCR amplification were the following: 94° C of denaturation, 60°C of annealing, and 72° of extension, proceeding for 30 cycles. Once the PCR reaction was complete, the samples were run on a 1.5% agarose gel and viewed under UV light. Densitometry was performed on the human epimorphin and GAPDH products. The human epimorphin product was verified through gel extraction, cloning (using a MiniPrep), and sequencing.

Results and Conclusions

In 2D cells, there was a slight increase of EPM expression in the T4 cells, compared with the rest of the stages (Figure 7). After performing densitometry, the expression levels were normalized with GAPDH levels, but the numbers did not seem to show a significant difference between the T4 expression and the rest of cells (Figure 8). However, in 3D, EPM expression in T4 cells was significantly higher than any of the other stages in the cell line (Figure 9). Again, the densitometry results did not seem to capture as much as a difference as it looks, but the T4 expression is nevertheless higher (Figure 10). In addition, the products were sent for sequencing, which verified that our product was human epimorphin. These results demonstrate that epimorphin could have a potential role in tumorigenesis in the mammary glands and, ultimately, in breast cancer. In the future, we would like to verify our results with a new series of cells following the HMT-3522 progression. We would also like to determine whether epimorphin contributes to the tumorigenic behavior of T4 cells by starting an invasion assay with T4 cells to see if an inhibitor against epimorphin blocks or inhibits invasion. Finally, we would like to look at human breast tumors for expressions of epimorphin by immuno-histochemistry.

Figure 7: RT-PCR 2D

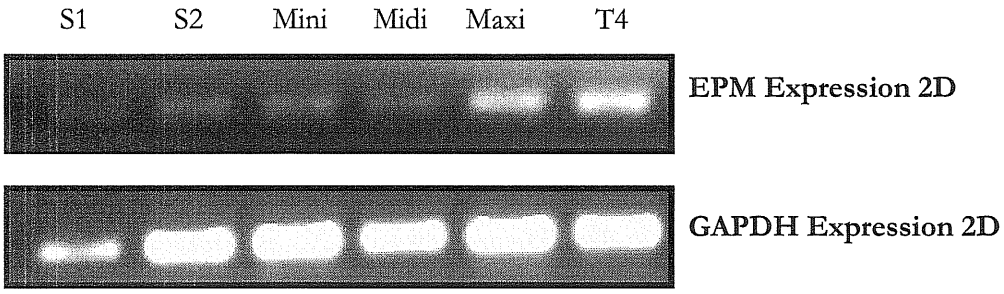

Figure 8: RT-PCR 2D Densitometry

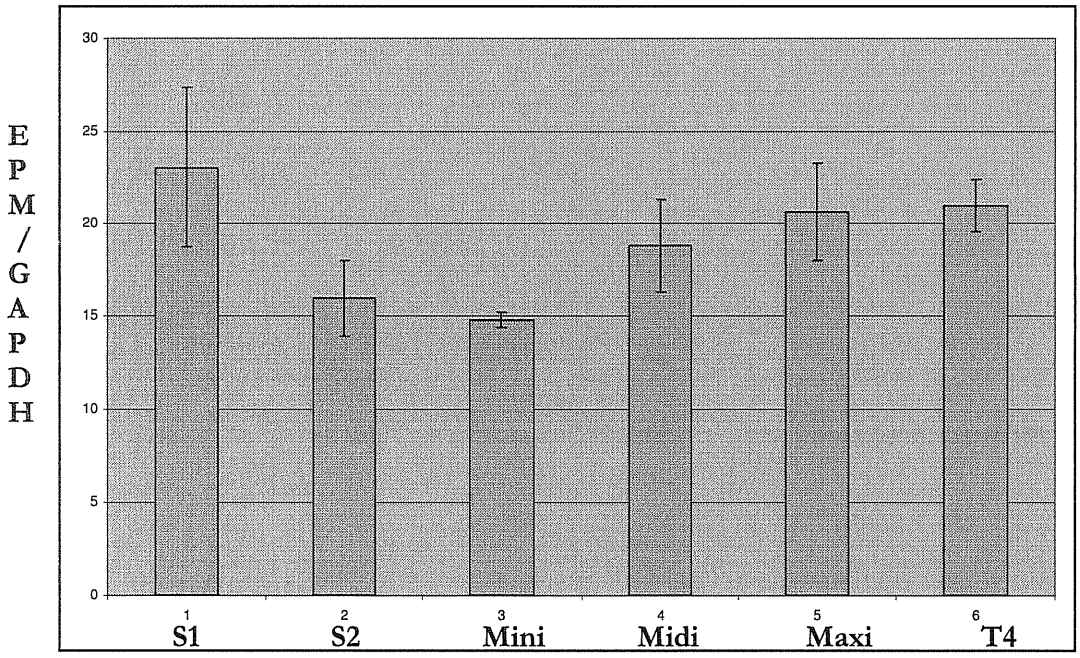

Figure 9: RT-PCR 3D

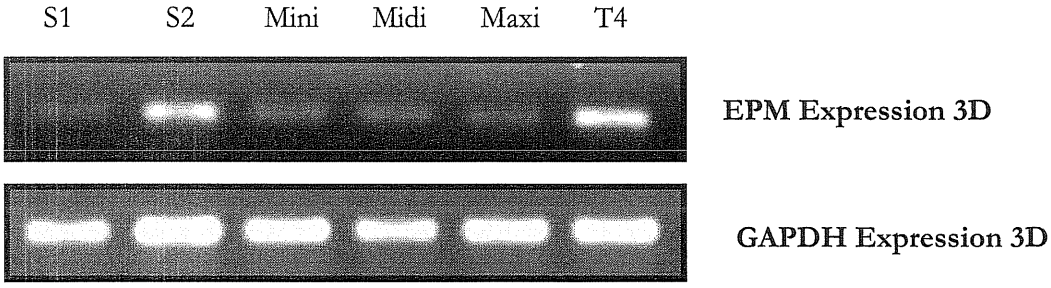

Figure 10: RT-PCR 3D Densitometry

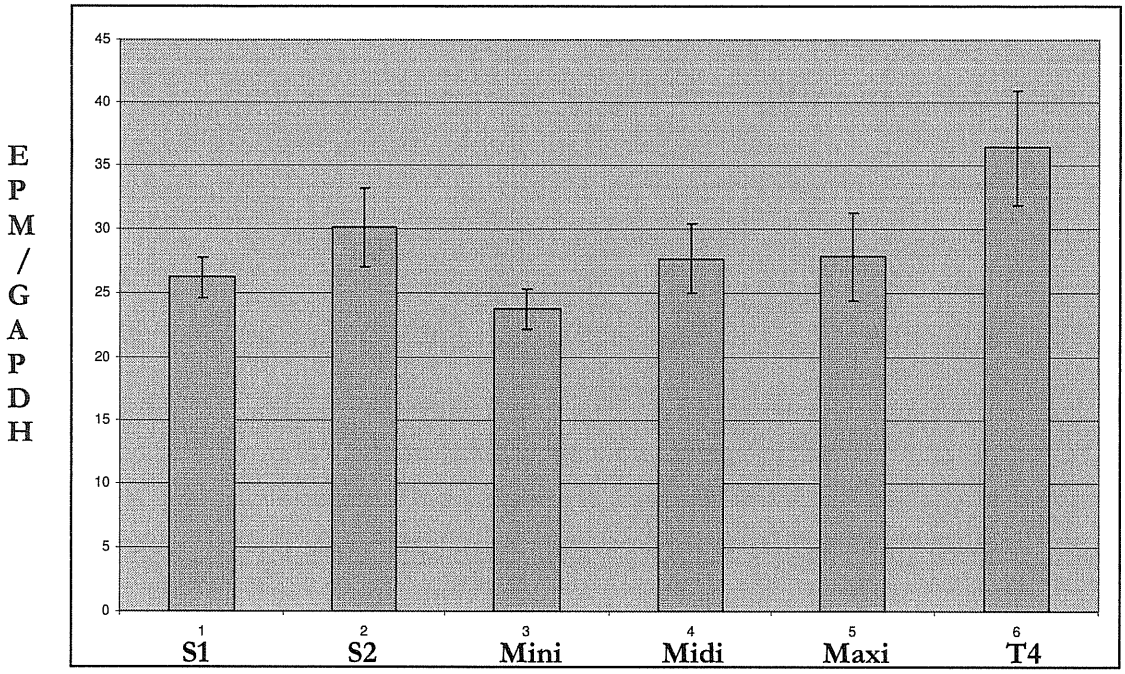

References

1. Hirai, Y., K. Takebe, M. Takashina, S. Kobayashi, and M. Takeichi. 1992. Epimorphin: a mesenchymal protein essential for epithelial morphogenesis. Cell. 69:471-481.
2. Radisky, D., Hirai Y., and M. Bissell. 2002. Delivering the message: epimorphin and mammary epithelial morphogenesis. Trends in Cell Biology. 13 (8): 426-434.
3. Bascom, J. Submitted.
4. Hirai Y. et al. 2001. Epimorphin mediates mammary luminal morphogenesis through control of C/EBPβ. Journal of Cell Biology. 153: 785-794.
5. Hirai, Y. 1993. Molecular cloning of human epimorphin: identification of isoforms and their unique properties. Biochem. Biophys. Res. Commun. 191: 1332-1337.
6. Peterson, O. W., Ronnov-Jessen, L., Howlett, A. R. and Bissell, M. J. 1992. Interaction with basement membrane serves to rapidly distinguish growth differentiation pattern of normal and malignant human breast epithelial cells. Proc Natl Acad Sci USA. 89: 9064-8.

Brateil Badal
Caroline Kane Lab
Project Title: Hepatitis C Virus

Introduction

Hepatitis C Virus (HCV) has infected 170 million individuals worldwide, 4 million of which are from the United States alone. HCV may eventually cause chronic infection, liver cirrhosis, and

hepatocellular carcinoma. While the direct cause is unknown, further investigation on the virus' replication process may provide insight into the cause of cancer, from the liver to the breast, by comprehending the regulation and dysregulation of the viral genes.

Currently there is no vaccine or cure for the virus, making it a hot subject for researchers to pursue. The viral RNA genome itself codes for only ten proteins, four structural and six nonstructural. In order for the virus to survive, it must successfully reproduce itself; therefore, the process of replication is a vital part of its life cycle. The protein responsible for copying the genome is the virus' polymerase, Nonstructural Protein 5B (NS5B). This RNA-dependent RNA polymerase is thought to interact with other nonstructural proteins to form a replication complex. One other protein in particular is NS3, the viral helicase and also protease. Only one paper has suggested a functional, physical interaction between NS3 and NS5B. My goal is to express and purify NS3 and the other nonstructural proteins so that we can assess their role in replication. Purification of these proteins may eventually allow us to build a replication complex *in vitro*. By doing so, we can then better understand the interactions of the viral proteins with NS5B and target essential replication mechanisms necessary for the virus to reproduce. If these essential mechanisms can be inhibited by drugs, then the virus cannot successfully be able to replicate itself.

Understanding HCV transcription regulation also could shed some light on other viruses and their regulation mechanisms, such as the bovine virus, or the mouse mammary tumor virus. These provide links specifically to the field of breast cancer but also would facilitate research in all types of cancer. Finally, studying expression or lack of expression of certain gene products can lead to cancer, i.e. oncogenes. This could be due to dysregulation of transcription. Therefore, researching transcription regulation allows us to better comprehend how specific protein production leads to cancer.

Methods and Results

Growth Curve for NS3 Overexpression

Determine the growth rate of *E. coli* BL21DE overexpressing NS3 by plotting an IPTG induced growth curve for NS3 and observe if the induction slows the growth of the transformed *E. coli*, suggesting that the non structural protein is being overexpressed.

Generate growth curves for:

- BL21DE
- BL21DE + IPTG
- BL21DE transformed with pA NS3
- BL21DE transformed with pA NS3 + IPTG

<u>Methods</u>

Day 1

1. Add 0.1% glucose to LB
2. Inoculate BL21DE in 3 mL LB using sterile technique.

3. Inoculate starter culture in 3mL LB and 3µL Cm (50µg/mL) for NS3 using 50 uL from the previous experiment's (1.8) starter cultures.
4. Grow O/N.

Day 2

1. Prepare 2 flasks with 100 mL of LB using sterile technique.
2. Add 100µL Cm (50µg/mL) into 1 of 2 flasks (NS3).
3. Inoculate **all 3 mL** from starter culture into each 100mL LB flask.
4. Take an aliquot at time zero before taking flasks to the warm room.
5. Grow cells for 5 hours in 37°C while shaking, and take **500 uL** alliquots every 30 minutes.
6. Before induction, split each 100mL flask into two 50 mL aliquots. Mix.
7. Before induction, take 20 uL sample of both
   a. BL21DE
   b. BL21DE+ pANS3
   (at time 150 from inoculation) and add 20uL of 2 x SDS sample buffer.
8. When OD600 is 0.4-0.7…
   a. add 1M IPTG to 1mM for the following cultures…
      1) BL21DE
      2) BL21DE pA NS3
9. Take a 500ul aliquot every 30 minutes.
   Blank Spectrophotometer with LB. Read Absorbance at 600.
10. Take time course aliquots of induced cells for SDS-PAGE loading.
11. Take 20uL samples at time 0, 60, 120, 180, 240 of NS3+IPTG, and 240 (BL21 Post Induction)
    Add 20µL bacterial sample (taken from the sample after OD was taken) to 20µL of 2X SDS sample buffer immediately to halt growth.

Results

Data Table 1:
OD Readings for BL21, BL21+ IPTG, BL21DE+pA NS2, BL21DE+pA NS2+ IPTG, BL21DE+pA NS3, BL21DE+pA NS3+ IPTG from time of inoculation and time from induction

Time	Time from Inocul. (min)	Time from induction	BL21	BL21+ IPTG	BL21DE+ pA NS3	BL21DE+ pA NS3+ IPTG
10:00am	0		.145	__	.135	__
10:30am	30		.195	__	.171	__
11:00am	60		.317	__	.247	__
11:30am	90		.589	__	.442	__
12:00pm	120	0	.686	692	.506	517
12:30pm	150	30	.902	.922	.693	.675
1:00pm	2:1 180	60	.658	.660	.504	.421
1:30pm	2:1 210	90	.694	.721	.626	.477
2:00pm	2:1 240	120	.760	.768	.688	.497

2:30pm	2:1 270	150	.796	.845	.737	.527
3:00pm	2:1 300	180	.833	.881	.775	.537
3:30pm	2:1 330	210	.891	.937	.841	.597
4:00pm	2:1 360	240	.910	.972	.880	.586

Data Table 2:

Undiluted OD Readings for BL21, BL21+ IPTG, BL21DE+pA NS3, BL21DE+pA NS3+ IPTG from time of inoculation and time from induction

Time	Time from Inocul. (min)	Time from induction	BL21	BL21+ IPTG	BL21DE+ pA NS3	BL21DE+ pA NS3+ IPTG
10:00am	0		0.145	__	0.135	__
10:30am	30		0.195	__	0.171	__
11:00am	60		0.317	__	0.247	__
11:30am	90		0.589	__	0.442	__
12:00pm	120	0*	0.686	692	0.506	517
12:30pm	150	30	0.902	0.922	0.693	0.675
1:00pm	180	60*	1.316	1.32	1.008	0.842
1:30pm	210	90	1.388	1.442	1.252	0.954
2:00pm	240	120*	1.52	1.536	1.376	0.994
2:30pm	270	150	1.592	1.69	1.474	1.054
3:00pm	300	180*	1.666	1.762	1.55	1.074
3:30pm	330	210	1.782	1.874	1.682	1.194
4:00pm	360	240*	1.82	1.944	1.76	1.172

Graphed Data:

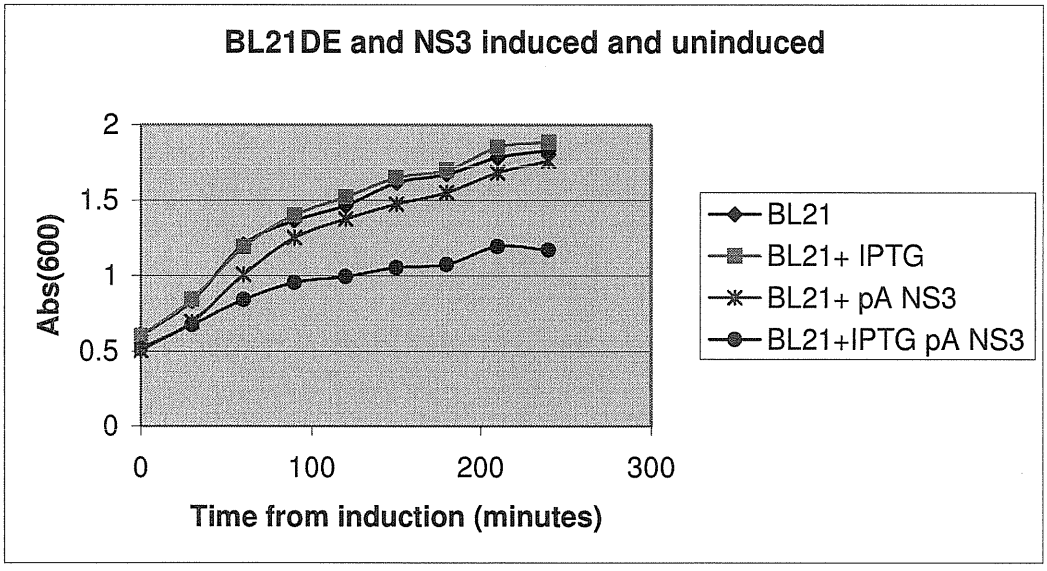

Analysis of NS3 Overexpression

Analyze expression of protein from induced *E. coli* BL21DE pACYC NS3 by SDS-Polyacrylamide Gel Electrophorisis (PAGE). Determine if NS3 is overexpressed in BL21DE. Determine the optimal period of expression of NS3 in the growth of BL21DE.

Plan:

1. Prepare the SDS-PAGE gel.
2. Stain proteins by Coomassie Brilliant Blue.
3. Observe expression of NS3 (69kDa).

Methods

1. Make the SDS gel
    a. Prepare 5mL 10% SDS-PAGE Resolving Gel
    b. 1.25 mL 5% SDS-PAGE Stacking Gel
2. Determine how much cell extract to load: 10 uL per lane
3. Obtain the following samples:
    a. BL21 + pA NS3, 0 min (preinduction)
    b. BL21 + pA NS3 + IPTG, 60 min
    c. BL21 + pA NS3 + IPTG, 120 min
    d. BL21 + pA NS3 + IPTG, 180 min
    e. BL21 + pA NS3 + IPTG, 240 min
    f. BL21, 0 min (preinduction)
    g. BL21 + IPTG, 60 min
    h. BL21 + IPTG, 120 min
    i. BL21 + IPTG, 180 min
    j. BL21 + IPTG, 240 min
    k. BL21, 240 min
    l. Molecular Weight Marker
4. Add 2x SDS loading buffer to 1x in each sample (completed in Expt 1.1).
5. Incubate samples at 100°C for **20 minutes**. Remove and place into ice.
6. Load samples using loading tips. Make sure to fully expel all protein into wells, then wash tip out by pipetting in and out 3-4 times with running buffer.
7. Run at 90V while Bromophenol Blue is in the stacking gel. Run at 120V when the Bromophenol Blue gets to the resolving gel. Stop when Bromophenol Blue travels to the bottom edge of the gel.
8. Place resolving gel in Tupperware (drawer A3) and stain with Coomassie Brilliant Blue R-250 solution by covering gel. Place on orbital shaker at 55 rotations for 1 hr.
9. Destain gel in destaining solution until bands can be seen. Add chemwipes (in a ball) to destaining solution to removing Coomassie from solution. Pour solution down sink and obtain completed gel.

Results

SDS-PAGE - Lanes **(left to right)**

1. BL21 + pA NS3, 0 min (preinduction)
2. BL21 + pA NS3 + IPTG, 60 min

3. BL21 + pA NS3 + IPTG, 120 min
4. BL21 + pA NS3 + IPTG, 180 min
5. BL21 + pA NS3 + IPTG, 240 min
6. BL21, 0 min (preinduction)
7. BL21 + IPTG, 60 min
8. BL21 + IPTG, 120 min
9. BL21 + IPTG, 180 min
10. BL21 + IPTG, 240 min
11. BL21, 240 min
12. Molecular Weight Marker

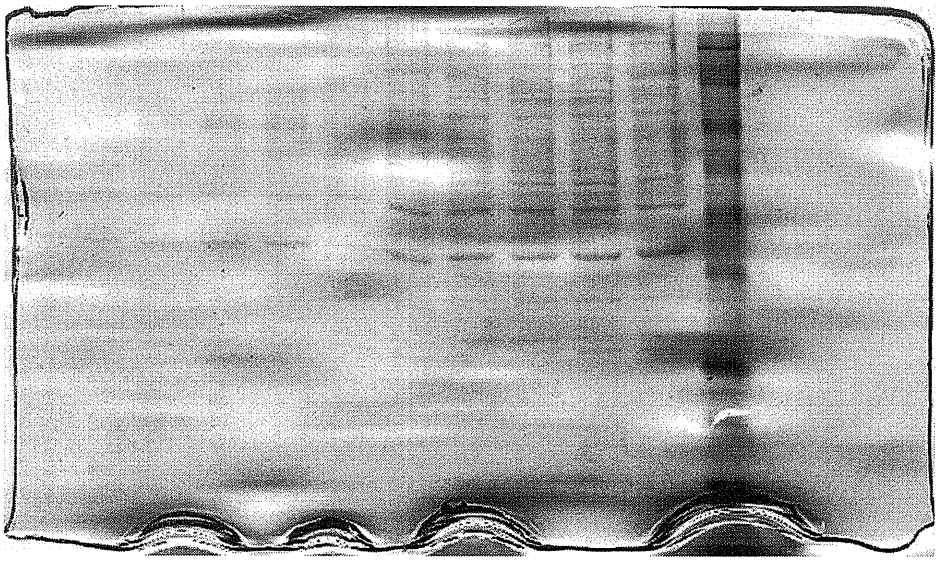

Examination of the SDS-PAGE gel showed possible evidence of expression of NS3 in transformed BL21DE induced with IPTG. There was a band at 69 kDa, approximately 64.2 kDa on the gel (the pink dyed marker protein) for NS3.

Purification of NS3

Pilot expression and purification of NS3 from BL21DE transformed with pACYC NS3; determine if NS3 is being expressed after induction with IPTG and determine if expressed NS3 is soluble.

Methods

Day 1

1) Inoculate starter cultures (Caroline): Grow O/N in 37°C room.
    a) BL21DE transformed with pACYC NS3 (colony from 6.19.05 plate in 4°C)

Day 2

2) Inoculate **2ml** of starter cultures into 100mL LB flasks.
3) Add 0.1% glucose (500 uL glc/ 100 mL LB)
4) Grow at 37C.
   Take 1 mL samples for OD readings.

Time	Inoculation (min)	Induction (min)	BL21DE+ NS3 Abs (600)	BL21DE+ NS3+ IPTG Abs (600)
11:55 am	0		0.196	
12:05 pm	20		0.202	
12:25 pm	40		0.264	
12:45 pm	60		0.387	
12:53 pm	67		0.484	
1:05 pm	79	0	0.495	0.502
4:05 pm	259	180 (3 hrs)	1:4 dilution 0.621→ 2.484	0.370→ 1.480

5) Grow cultures at **30°C** (to make NS3 more soluble) for 3 hours. Read OD600
6) Take 1mL sample of BL21DE pACYC NS3 and BL21DE + IPTG each.
7) Aliquot the rest of BL21DE pACYC NS3 + IPTG into prechilled yellow cap GSA bottles
8) Spin cells for 10min at 1600g (10,000rpm GSA rotor) at 4C
9) Decant supernatant
10) Flash Freeze cell pellet at -70C (liquid nitrogen from -80°C room)

Day 3

1) Pre-chill buffer 1
2) Assume 1mL of E.coli at OD 600 = 1.0 gives ~ 2mg of wet cells.
3) Resuspend 1g of wet cell pellet in 3-5 mL of buffer 1 in **25 mL conical tube**.

Test NS3 solubility

1) Incubate cells at 4°C for 30 min.
2) Sonicate on ICE
   a. Sample must be in 25mL conical. In beaker with ice-salt (we didn't add salt – no grainy salt found)
   b. microtip sonciator – keep in beaker with ice when not sonicating to keep tip cold (it warms up by vibrating)
      1) **40% output.** Sonicate for 10 seconds, then 30 sec rest. Repeat **9** more times.

Total fraction

3) Remove 20ul sample and add 20ul 2x SDS protein gel loading buffer.
4) Spin down 60ul for 15 min at 4C 12000rpm.

Soluble fraction

5) Obtain 20ul of supernatant. Add 20 ul 2x SDS protein gel loading buffer.

Pellet fraction (insoluble fraction)

6) Obtain cell pellet alone.
7) Resuspend pellet in 20ul of buffer 1, and add 20ul 2x SDS loading buffer.

Test Ni-NTA binding

1) Equilibrate Ni-NTA resin (slurry) -100ul at **4C**
2) Obtain 100ul cell suspension in Buffer 1
3) Spin down at 4C 12000rpm for 15 min.
4) Transfer supernatant to 200ul slurry of pre-equilibrated Ni-NTA beads
5) Rotate at 4C for 1 hour. Spin down for 15 sec in picofuge.

Flowthrough (unbound fraction)

6) Aliquot supernatant into tube. Add 20 ul 2x SDS protein gel loading buffer
7) Wash resin (matrix/beads/substance that protein binds to) 3x with 200ul buffer 1

Eluate

8) Elute
    a. Add 110ul of buffer 2
    b. Incubate 5 min
    c. Spin down 10 sec in picofuge
    d. Recover supernant (eluate)
9) Take 20ul sample of eluate. Add 20 ul 2x SDS protein gel loading buffer.

Make Gels

1. Make one SDS-PAGE gel
    a. 5mL 10% SDS-PAGE Resolving Gel
    b. 1.25 mL 5% SDS-PAGE Stacking Gel

Day 4

Coomassie Stain Gel

1. Load samples (**17 uL of each**).
    1. Molecular Marker
    2. NS3 Pre Induction NO IPTG
    3. NS3 Post Induction NO IPTG
    4. Total fraction
    5. Soluble fraction
    6. Pellet fraction
    7. Flowthrough
    8. Eluate
2. Run at 80V while the BϕB is in the stacking gel. Run at 100V when the BϕB gets to the resolving gel. Stop when BϕB is at very bottom edge of the gel.
3. Stain resolving gel in Coomassie Brilliant Blue R-250 solution, for 1 hr.
4. Destain gel in destaining solution until bands can been seen. Add chemwipes to destaining solution.

Results

NS3 Purification Gel (left to right)

Lane1: Molecular Marker
Lane 2: NS3 Pre Induction NO IPTG
Lane 3: NS3 Post Induction NO IPTG

Lane 4: Total fraction
Lane 5: Soluble fraction
Lane 6: Pellet fraction
Lane 7: Flowthrough
Lane 8: Eluate

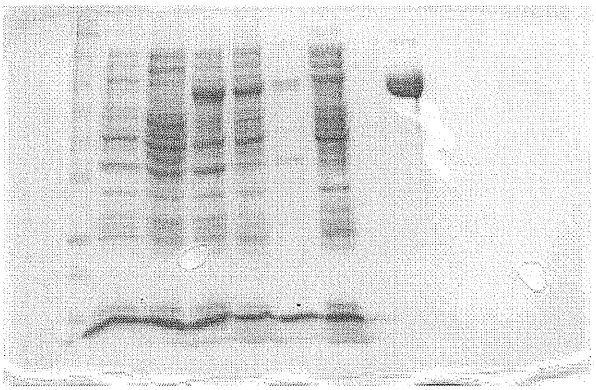

A faint band was seen in the eluate at the 69 kDa mark, showing that NS3 was purified; however, a better technique will be used with the next NS3 purification experiment so that more protein can be made and made soluble, and also so that more can be loaded.

Tanya Egodage
Mina Bissell Lab
Supervisor: Jimmie Fata
Project Title: MMP-3 mediated responses in breast epithelial cells

Background

Historically, tumor necrosis factor (TNF) has been characterized for its tumor necrotizing effects. However, it has recently been extensively researched for its ability to induce apoptosis in abnormal cells. TNF was originally assumed to be a macrophage and subsequently named the tumor necrosis factor. Following that, a different group of scientists discovered another factor named lymphotoxin (LT). After comparison of these two ligands, their homology was determined, and they came to be known as TNFa and TNFb, with TNFb being LTa. These two became the first ligands characterized in the tumor necrosis superfamily, which currently describes a group of 29 membrane ligands. The TNFa superfamily ligands and receptors have been shown to be involved in a variety of cellular responses, including apoptosis, survival, differentiation, or proliferation (through induction of proteins such as NF-KB, JNK and MAPK) of cells. It has also been implicated in a variety of diseases.

Cell survival and normal proliferation exists as an interplay between the two pathways that TNF it can catalyze: the survival pathway or the death pathway. The pathway of a wild type cell maintains survival through induction of NFkB, while aberrations in cell function stimulate the death pathway through intermediates including c-Jun NH2-terminal kinase (JNK).

Another factor involved in the regulation of survival or death of a cell is p53. From its discovery twenty-five years ago, the p53 gene has been of significant interest to the scientific and medical community. Mutations in this gene have been documented in over half of the cancers diagnosed by doctors. The p53 protein is a transcription factor that acts as a tumor suppressor, normally inducing apoptosis of the cell with abnormal cellular activity. Mutation in the p53 gene, therefore, results in abnormal proliferation of the cell. p53 has also been widely documented in breast carcinomas, and is the causative factor in the Li-Fraumeni syndrome.

In certain cell lines, p53 has been determined to be induced in TNFa- induced apoptosis. Those studies imply that TNFa can induce NFKB, which can subsequently up-regulate p53.

Introduction

Previously, the TNFalpha superfamily has been shown to induce apoptosis under abnormal cell conditions. The TNF pathway can be described by two pathways: a survival pathway, and a death pathway. Under normal cell activity, the TNF pathway induces NFkB, and leads to the survival of the cell. However, under stress or abnormal cell growth, the TNF pathway diverts to the death pathway, leading to apoptosis, or programmed cell death. The understanding of the relationship and mechanism of these two pathways is largely superficial.

One of the members of the TNFa superfamily includes TNF receptor apoptosis inducing ligand (TRAIL). In preliminary studies, TRAIL has been implicated in the blebbing pathway induced by matrix metalloprotease 3 (MMP3). MMP3 has been shown to induce the NFkB pathway to stimulate cell survival, as well as induction of caspases to stimulate cell death. It is currently unclear where TRAIL functions; it is hypothesized that its function lies downstream of MMP3 before the decision to enter the survival or cancerous pathway of MMP3. Addition of cyclohexamide (CHX) induces the death pathway regulated by MMP3.

A related pathway involves the p53 protein, which is transcribed from the p53 gene. Many breast carcinomas display a mutation in the p53 gene, as do many other types of cancers. However, in mammary epithelial tissue, it has yet to be determined whether the regulation of this p53 product occurs at the transcriptional or translational level.

The specific characterization of the concentrations of TNFa members as well as their interaction with p53 have been only superficially investigated. Understanding this mechanism to a greater extent would provide great insights into the understanding of breast carcinomas and treatments thereafter.

Another factor, named neocarzinostatin (NCS), has antiproliferative activities, and has been shown, in certain organisms, to induce DNA damage.

Materials and Methods

The following is a summary of the procedures necessary to initiate investigation of the aforementioned mechanisms.

Initial experimentation will involve the screening of the TNFalpha superfamily members through PCR screening. The gene of interest includes the genes for each of the members of the TNF alpha superfamily. Following the design of primers, both the forward and reverse primers will be obtained for each gene of interest. The primers will then be utilized with the complementary DNA obtained from S1 cells. The primers that display bands in the area corresponding with the gene of interest will be documented. These primers demonstrate the genes expressed in the S1 cell lines. Each of these experiments will be finalized through an agarose gel electrophoresis.

Experimentation will also include the culturing of human MCF10A and mouse EPH4 cell lines on plastic. The human cell line will be obtained from a breast carcinoma from a patient at the University of California, San Francisco. Protein and RNA will be isolated and detected through Tripure techniques and Western blotting.

To confirm the prediction that TRAIL can induce blebbing of MCF10A cells, colonies will be treated with cyclohexamide, a reagent that cleaves extracellular receptors, shutting off the cellular machinery. MMP3 will be used as a control to demonstrate blebbing, while further samples will be treated with SHAM, the serum in which MMP3 is incubated, as well as varying concentrations of TRAIL. The optimum concentration of TRAIL necessary to induce blebbing will be determined by repeating this experiment.

A final experiment will be conducted, and protein samples will be collected and shown through Western blotting.

Isolated RNA samples will also be quantified through quantitative real-time PCR, to determine relative amounts of RNA in each of the cell colonies. Isolate protein and RNA from samples of human MCF10A and mouse EPH4 cell lines treated with TNFa, and the receptors.

The cDNA made from RNA collection of the EPH4 cells will be amplified through PCR, using mouse-specific primers, and visualized after agarose gel electrophoresis.

In addition to these experiments, MCF10A cells will be cultured and treated with neocarzinostatin (NCS), an antiproliferative agent that can cause DNA damage in some organisms, through a time-lapse experiment lasting 24 hours. Protein from these samples will be identified through Western blotting. RNA and protein quantities of the p53 protein will be compared, to determine the level at which it is regulated.

Results

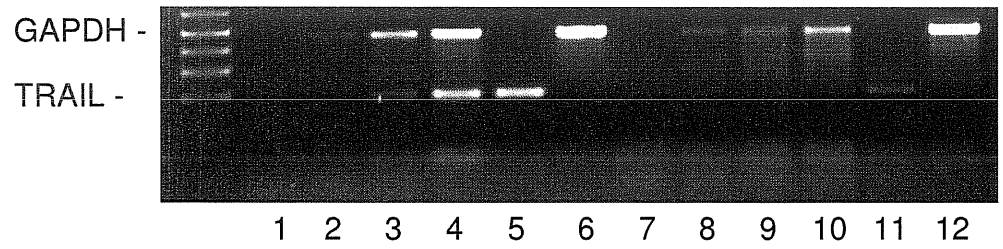

Figure 1. TRAIL and GAPDH primers with MCF10A (lanes 1-6) and S1 cells (lanes 7-12) at varying cycles. TRAIL is expressed only on the MCF10a cells and not on S1 cells, so it may be involved in the apoptotic pathway leading to blebbing of the cells.

Ligand	Expressed in MCF10A	Expressed in S1
EDA-A2	No	
BAFF	Yes	
APRIL	No	
GITRL	No	
OX40L	No	
41BBL	No	
CD40L	No	
CD30L	No	
CD27L	No	
LIGHT	No	
RANKL	Yes	
TRAIL	Yes	No
EDA-A1	Yes	
TNFa	Faintly	
LYMPHO	Yes	

Table 1. Summary of RT-PCR results from the TNFα superfamily ligand screening experiment.

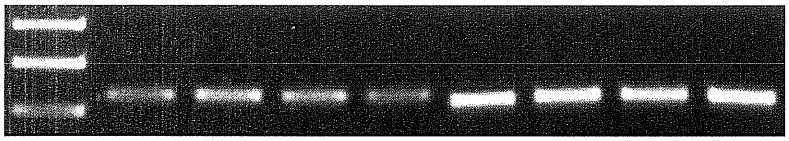

Figure 2. p53 primer optimization. Lanes 1-4 show primer 1, lanes 5-8 show primer 2.

Michelle Lu
Daniel Koshland Lab
Supervisor: Evette Radisky
Project Title: Investigating mesotrypsin and SPINK1

Introduction

The development of a malignant phenotype and invasion of a tumor requires the activity of proteases. In malignant processes, the delicate balance between production, activation, and inhibition of proteases is often irreversibly disturbed. There is evidence that a critical step in cancer growth and metastasis requires the dissolution of the extracellular matrix surrounding the malignant tumor, which leads to tumor cell invasion and dissemination [1]. Different isoforms

of trypsinogens, a subgroup of the matrix serine proteases (MSPs), can degrade collagen in the extracellular matrix and can also activate other proteases such as the matrix metalloproteases (MMPs) which also play an important role in cancer progression.

Using a 3D tissue culture model of breast cancer, it has been found that the treatment of these cells with serine protease inhibitors suppress malignant growth. Furthermore, it was found that gene expression of mesotrypsin, an isoform of trypsin, was greatly enhanced in tumorgenic cells in this model. Mesotrypsin is a unique enzyme resistant to inhibition by endogenous SPINK1 trypsin inhibitor that is also expressed in breast cancer cells.

The goals of this research will include cloning, expressing, and purifying mesotrypsin and the inhibitor SPINK1 for biochemical and structural studies, towards developing mesotrypsin inhibitors that will potentially suppress malignant growth and be therapeutically useful.

Materials and Methods

Materials. A SPINK1 expression construct was obtained from E. Radisky (UC Berkeley). A mammalian expression construct for mesotrypsin was obtained from N. W. Bunnett (UCSF). PET-26b (+) vector was supplied by Novagen. The restriction enzymes Dpn I, MSC I, XHO I were supplied by New England Biolabs. T4 ligase and calf intestinal alkaline phosphatase were supplied by Invitrogen. For all PCR reactions, cloned Pfu Polymerase and buffer were supplied by Stratagene.

E.Coli Transformations, Cell Cultures, DNA isolation, and DNA quantitation. SPINK1 and mesotrypsin expression constructs were transformed into Invitrogen One Shot TOP10 chemically competent cells through heat shock following the manufacturer's instructions. The transformed TOP10 cells were plated onto LB + kanamycin and grown overnight at 37 °C. Colonies from the plates were cultured in LB+kan at 37 °C, and then DNA was extracted using Qiagen Qiaprep Spin Miniprep or Qiagen Hi Speed Plasmid Maxiprep kits. DNA concentrations were determined by UV absorbance using an HP 8453 UV/Vis spectrophotometer and chemstation software.

Sequencing. All sequencing was executed by the UC Berkeley Sequencing Lab. For the mesotrypsin sequencing, the T7 promoter and terminator primers were used at 3.2 picograms in addition to 0.5 micrograms of the mesotrypsin DNA in a total volume of 13 microliters. For the SPINK1 mutants sequencings, the T7 terminator primer was used at 3.2 picograms plus 0.5 micrograms of the SPINK1 DNA to a total volume of 13 microliters. EditView, FourPeaks, and/or FinchTV were used to view the chromographs of the reactions. ClustalW was used for sequence alignment for both nucleic and aminoacid sequences. An Expasy online translating tool was used for translation.

Digestion and Ligation. The obtained mesotrypsin gene was harbored in the vector pcDNA3.1 (+). Restriction digests were carried out at 37 °C for three-hours to overnight using buffers supplied by the manufacturer. Ligation reactions were carried out at 16 °C using the conditions specified by the manufacturer. Digested vector was treated with calf intestinal alkaline

phosphatase (CIAP) to reduce the background of religated vector. Qiagen's PCR Purification Kit was used on digested products.

Agarose Electrophoresis. All DNA samples were electrophoresed in 1% (w/v) agarose gels, in a mini-gel system (Bio-Rad) using TAE buffer and ethidium bromide staining.

PCR Mutagenesis . Point mutations were introduced into the SPINK1 gene using Quick-change Site-Directed Mutagenesis protocol (Stratagene). Primers were designed according to the manufacturer's guidelines to achieve a melting temperature equal to or greater than 76 °C. PCR was carried out in a PTC-100 programmable thermal controller (MJ Research) for 12 cycles of the following: 30sec at 95 °C for denaturing, 1 min at 55 °C annealing, and 11min at 68 °C for extension. The sequences of the oligonucleotides and their Tm are as follows:
1) GGAGATATACATATGGGCATGGAAGCGAAATGTTATAAC with a melting temperature of 67.85 °C
2) GAAGCGAAATGTTATAACGAATTGAACGGGTGTACC with a melting temperature of 68.09°C
3) GTCAAACATCTATTCTGATTCAGAAAAGCGGTCCATGC with a melting temperature of 69°C

Expression strains and growth. The final mesotrypsin and SPINK1 constructs were transformed into Novagen Rosetta 2 Singles and BL21(DE3)pLysS Singles competent cells. Protein expression was induced with IPTG.

Cell fractionation. Harvested BL21 cells were subjected to sonication using Heat Systems—Ultrasonic, inc.'s Sonicator Cell Disrupter. Cells were lysed and periplasmic, cytoplasmic, and insoluble protein extracts were collected.

Denaturing protein gels. All protein extracts were electrophoresed in denaturing 8% SDS gel at 100Volts in a Bio-Rad minisystem. TEMED was supplied by Sigma and 30% acrylamide/bis solution was supplied by BioRad. Coomassie staining followed electrophoresis, and an overnight acetic acid destaining was performed on the stained gel.

Results

Mutagenesis of SPINK1

A pET27 construct containing the SPINK1 synthetic gene was transformed into TOP10 cells and multiple transformants were miniprepped and sequenced. Sequencing revealed many mutations. To obtain the desired SPINK1 sequence, the Quickchange Site-Directed Mutagenesis protocol was applied to each of the three point mutations identified in the SPINK1 clone containing the fewest mutations. This method of PCR-amplification of the entire plasmid using complementary forward and reverse primers, both containing the desired substitution. The PCR products of each mutagenesis were then subjected to DpnI digestion to eliminate all parental plasmid DNA, and transformed into TOP10 competent cells. Following each round of mutagenesis, several transformants were miniprepped and sequenced, and a clone containing the desired mutation was

selected for further work. After completion of the final round of mutagenesis, the plasmid incorporating all desired mutations was prepared on a larger scale by maxiprep.

Subcloning of Mesotrypsin

The mesotrypsin gene was harbored in the eukaryotic expression vector pcDNA3.1(+). In order to have the mesotrypsin sequence follow a bacterial promoter and secretion sequence necessary for protein expression and periplasmic localization in E. coli, the mesotrypsin gene was subcloned into the vector pET-26b (+). The desired insertion location fell between the MscI and XhoI restriction sites of the pET-26b(+) vector, but the mesotrypsin gene contained only the XhoI site at its 3' end. The mesotrypsin gene was PCR amplified using a 3' primer containing the XHOI site and a 5' primer that introduced an MscI site. The PCR product and the pET-26b(+) vector were both digested with MscI and XhoI. The digested pET-26b(+) plasmid was treated with CIAP to reduce the background of re-ligated vector. The digested products were both purified using Qiagen PCR purification kit. The purified digested products were then ligated in a 1:1 and 1:4 ratio. The incorporated mesotrypsin gene was verified through sequencing. The new expression construct was prepared on a larger scale by maxiprep.

Expression Studies

The SPINK1/pET-27 and mesotrypsin/pET-26 constructs were transformed into BL21(DE3) pLysis cells for expression studies. After inducing protein expression with IPTG (and no IPTG for controls), the cells were fractionated into periplasmic, cytoplasmic, and insoluble fractions. The protein extractions were run on SDS page gels to determine whether or not mesotrypsin and SPINK1 were successfully expressed. A band of 28.9 kDa was found in the mesotrypsin induced insoluble fraction (Figure 1). This band of 28.9 kDa corresponds to the size of mesotrypsin gene plus the signal sequence. No other fractions contained bands corresponding to the molecular weight of mesotrypsin or SPINK1.

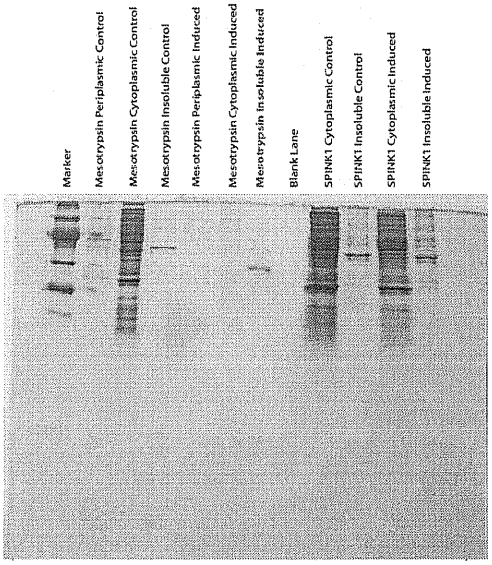

Figure 1. SDS gel of cell fractions.

Discussion

The rounds of mutagenesis of SPINK1 were successful, and the subcloning of mesotrypsin into the pET-26b(+) vector went smoothly. After two months of cloning and mutagenizing, mesotrypsin and SPINK1 were ready for expression studies.

Both pET vectors contain a signal sequence, which when put downstream of the insert, should result in protein localization in the periplasmic space. The denaturing gels did not show any bands corresponding to mesotrypsin or SPINK1 in the periplasmic fraction. However, the insoluble fraction of the mesotrypsin-containing cell extracts did show a band the size of mesotrypsin plus the signal sequence. This indicates that mesotrypsin was successfully expressed, but not localized to the periplasmic space. The presence of the signal sequence still attached to the mesotrypsin protein suggests that the sequence was not recognized and transported to the periplasmic space where the signal sequence would be cleaved, which may be due to improper folding of the mesotrypsin protein. It seems that mesotrypsin is being retained as an insoluble inclusion body, improperly folded.

There were no bands in any of the fractions that corresponded to SPINK1, indicating that SPINK1 is not being expressed at all.

Future directions may include optimizing secretion of the proteins in different constructs or under different conditions, or, purification and refolding of the proteins from inclusion bodies.

References

1. Merja Moilanen et al. "Tumor-Associated Trypsinogen-2 (Trypsinogen-2) Activates Procollagenases (MMP-1, -8, -13) and Stromelysin-1 (MMP-3) and Degrades Type I Collagen." *Biochemistry* 42 (2003): 5414-5420.

KEY RESEARCH ACCOMPLISHMENTS

- **Andrew Lee** (Nandi Laboratory) examined the effect of estrogen supplementation on genes associated with breast cancer in a rat model.
- **Carol Li** (Bissell Laboratory) successfully established a TGF-beta responsive promoter reporter construct and expressed this construct in mammary epithelial cells.
- **Deepti Nahar** (Bissell Laboratory) validated gene expression data from microarray experiments showing differential expression of genes involved in double-strand break repair at both the RNA and protein levels.
- **Jason Ahn** (Bissell Laboratory) investigated the role of MT1-MMP in the branching stage of mammary gland morphogenesis.
- **Neda Roosta** (Bissell Laboratory) examined the gene expression levels of epimorphin in a human breast cancer progression series.
- **Brateil Badal** (Kane Laboratory) successfully over-expressed and purified the NS3 hepatitis C helicase and protease protein.

- **Tanya Egodage** (Bissell Laboratory) analyzed the expression of TNFa ligand superfamily members in MCF10A cells.
- **Michelle Lu** (Koshland Laboratory) successfully cloned mesotrypsin and its inhibitor, SPINK1.

REPORTABLE OUTCOMES

Deepti Nahar, Jason Ahn, Brateil Badal, and **Tanya Egodage** graduated from UC Berkeley in the past academic year with B.S. degrees. As of yet, no patents or publications have derived from this work.

CONCLUSIONS

The third and final year of the undergraduate research training program was equally as successful as the two previous years. Many of the summer trainees stayed on in their training labs during the following academic year on a volunteer basis. Several manuscripts, currently in preparation, contain experimental results produced by the undergraduate trainees. This program provided valuable training and experience for the undergraduate students in performing directed academic research.

This program was designed to recruit qualified undergraduates with an interest in research, and to provide them with a highly interactive program that integrated the unique expertise available in our laboratories in the Life Sciences Division of the E.O. Lawrence Berkeley National Laboratory and the Department of Cell & Molecular Biology at the University of California, Berkeley, and to guide them towards developing an interest in investigating the underlying mechanisms involved in the development of breast cancer. Trainees in the program benefited from working in a dynamic environment that investigates issues at the forefront of breast cancer research. The students chose from projects investigating the effects of hormones on mouse mammary glands, the role of extracellular matrix and soluble factor signaling in cellular behavior, and dissecting viral transcriptional regulation. Projects were designed with a goal towards cohesive research objectives that were meaningful, educational, and attainable. Students were matched with a postdoctoral fellow or a staff member conducting research relevant to their projects and worked closely with their supervisors and reported regularly on their research progress to the larger training group.